AN ABSTRACT OF THE THESIS OF

Brendan M. Rogers for the degree of Master of Science in Environmental Sciences presented on July 31, 2009.
Title: Potential Impacts of Climate Change on Vegetation Distributions, Carbon Stocks, and Fire Regimes in the U.S. Pacific Northwest.

Abstract approved:

Ronald P. Neilson Beverly E. Law

The U.S Pacific Northwest contains a wide variety of ecosystems, all subject to relatively dry summers and wet winters. As has been shown with paleoclimatic and paleoecological data, the region is vulnerable to changes in climate. We assessed the sensitivities of vegetation distributions, carbon stocks, and fire regimes to 21st century climate change by running MC1, a dynamic general vegetation model, over a large domain across Oregon and Washington at 800-meter resolution. During the historical period, MC1 generally overestimated carbon stocks in the Western Forests region and underestimated carbon stocks in the Eastern Forests and Columbia Plateau. MC1 displayed a strong bias in the seasonality of NPP towards decreased summer and increased winter production. This suggests the model's productivity equations may be overly sensitive to low soil moisture and under-sensitive to low temperatures. We downscaled nine future climate projections from three General Circulation Models (CSIRO Mk3, MIROC 3.2 medres, and Hadley CM 3), each run through three CO_2 emission scenarios (SRES B1, A1B, and A2). Temperatures increased ubiquitously and concurrently with increasing emission scenario, but precipitation was more varied. CSIRO climates were relatively cool and wet, MIROC climates were hot and wet, and Hadley climates were hot and dry. Precipitation generally increased in winter and decreased in summer, and temperature increases were highest in summer. Previous work showed that CSIRO performed poorly, MIROC moderately well, and Hadley very well in the Pacific Northwest for the historical period. Future climate projections amplified the seasonal trends in climatic variables, water stress, and productivity. MC1 simulated the Pacific Northwest's western maritime forests as being vulnerable to large increases in fires, subsequent losses in carbon stocks, and encroachment from more southerly and/or easterly forest types. The arid, fire-adapted

forests east of the Cascade appeared to be resilient to climate changes under MC1. With increasing precipitation, MC1 simulated vast expanses of shrublands in the Columbia Plateau and Northern Basin converting to grasslands or woodlands. Across the domain, MC1 runs under the CSIRO climate projections averaged 82% increases in biomass combusted and 1.2% (0.1 Pg C) decreases in ecosystem carbon, while those under MIROC averaged 22% increases in biomass combusted and 0.8% (0.07 Pg C) increases in ecosystem carbon. Climate projections from the Hadley model resulted in the most extreme changes, averaging 259% increases in biomass combusted and 15% (1.26 Pg C) decreases in ecosystem carbon. Our study suggests some areas within the Pacific Northwest may be vulnerable, and others resilient, to climate change, although this is highly dependent on model assumptions and uncertainties.

Potential Impacts of Climate Change on Vegetation Distributions, Carbon Stocks, and Fire Regimes in the U.S. Pacific Northwest

by
Brendan M. Rogers

A THESIS

submitted to

Oregon State University

in partial fulfillment of
the requirements for the
degree of

Master of Science

Presented July 31, 2009
Commencement June 2010

Master of Science thesis of Brendan M. Rogers presented on July 31, 2009.

APPROVED:

Co-Major Professor, representing Environmental Sciences

Co-Major Professor, representing Environmental Sciences

Director of the Environmental Sciences Program

Dean of the Graduate School

I understand that my thesis will become part of the permanent collection of Oregon State University libraries. My signature below authorizes release of my thesis to any reader upon request.

Brendan M. Rogers, Author

ACKNOWLEDGEMENTS

I would first like to thank my major advisor, Ronald Neilson, for his vision, guidance, feedback, and support over the last two years. I also can't speak highly enough of his support crew, the MAPSS team, and appreciate all the insight and technical help they've provided. Ray Drapek guided my first-year script writing and downscaling, Jim Lenihan taught me how to run MC1 and was always available for discussion, and John Wells was eager to help with any systems issues. Without them, this work would have easily dragged on for another year.

A number of other professors and fellow students offered valuable feedback on my work and added tremendously to my intellectual development at Oregon State. Although interactions with my co-advisor, Beverly Law, were relatively infrequent, they were packed with insightful and helpful comments that significantly shaped my research. She provided some great feedback on this thesis, and her lab also contributed some crucial datasets for calibration and validation. Dominique Bachelet has been one of the most eager, helpful, and supportive people during my Masters tenure, and I remain indebted and touched by her interest and help in my research. I am also very appreciative of Dave Conklin's assistance in fixing and augmenting any code errors that cropped up. My co-worker, Maureen McGlinchy, has proceeded with me step-by-step through this work, and I am thankful for her ideas, help, and friendship. I remain grateful for the quick and effective support our systems administrator, Terralyn Vandetta, offered time and time again, including on weekends. The PRISM group, led by Christopher Daly, has been very helpful in providing input historical climate data. I also would like to thank my other two committee members, John Bolte and Robert Harris, for their interest and feedback on my project.

Finally, I need to thank my family and new graduate school friends. Mike Messier, Garrett Meigs, Paul Satterthwaite, Maureen McGlinchy, Lauren Hall, Carlos Sierra, Steve Volker, Tiffany van Huysen, Travis Woolley, and many others turned times of gravity into times of levity, and I couldn't ask for a better group of friends. Along with supplying the majority of my calibration data, my wonderfully giving girlfriend, Tara Hudiburg, has offered tremendous emotional support. Lastly, I am forever indebted to my parents. My mother and father nurtured the intellectual curiosity that eventually landed

me in graduate school. And my stepmother, Karen, has been the most encouraging and loving stepparent one could ask for.

This research was supported by the U.S.D.A. Forest Service.

TABLE OF CONTENTS

LIST OF FIGURES

LIST OF TABLES

LIST OF APPENDICES

DEDICATION

To my father, an intellectual rebel, who passed away during the course of this research.

Potential Impacts of Climate Change on Vegetation Distributions, Carbon Stocks, and Fire Regimes in the U.S. Pacific Northwest

Introduction

The potentially momentous consequences of climate change are increasingly recognized nationally and internationally. Many studies report observed climate-induced changes in flora and fauna phenologies, species ranges, and fire occurrences (Walther et al. 2002, Root et al. 2003, IPCC 2007, CCSP 2007, Bowman et al. 2009). The topographically complex U.S. Pacific Northwest (PNW) contains a diverse range of vegetation types and fire regimes. On a per area basis, the PNW also contains some of the world's highest biomass forests and potentials for future carbon storage (Smithwick et al. 2002, Hudiburg et al. 2009). However, the PNW's ecosystems were sensitive to past climatic changes (Whitlock et al. 2003, Mckenzie et al. 2004, Gavin et al. 2007), are currently displaying evidence of (Miles et al. 2007, Mote et al. 2008) and responses to (Pierce et al. 2008, van Mantgem et al. 2009) climate change, and appear vulnerable to projected climate changes during the 21st century (Whitely Binder 2009). Sub-regions within the PNW may display different responses, which depend not only on changes in the means, but also in the variances and seasonal patterns of climatic variables (CCSP 2007). Yet there remains a lack of spatially explicit information on the sensitivity of the PNW to climate change at the sub-regional scale (Littell et al. 2009).

Over the last 20,000 years, the PNW has seen sizeable variations in fire return intervals and distributions of mesophytic and xerophytic taxa due to variations in Earth's orbit and consequent glacial extents (Whitlock 1992). The region's wet winters and dry summers render its ecosystems susceptible to increases in summer temperatures and related decreases in soil moisture (Miles et al. 2007, Climate Leadership Initiative 2008, Whitely Binder 2009). Our primary reference point for the region, the 20th century, displayed the wettest and least variable climate in the last millennium (Millar et al. 2006). However, climate is projected to change during the 21st century by magnitudes similar to or greater than those of the past 20,000 years, and at greater rates (Jackson and Overpeck 2000). Most climate projections include warmer, drier summers, even if annual precipitation increases (Mote et al. 2003, Climate Impacts Group 2004, Littell et al. 2009). Because of this, a number of studies have predicted substantial shifts in vegetation distributions (Bachelet et al. 2001, Shafer et al. 2001, Diffenbaugh et al. 2003) and

increases in fire occurrence (Thompson et al. 1998, Dale et al. 2001, Climate Leadership Initiative 2008, Blate et al. 2009, Elsner 2009).

There remain many questions regarding the magnitude, timing, and spatial extent of terrestrial ecosystem responses to future climate change in the PNW. For example, how will rising temperatures interact with the seasonality of precipitation to produce drought stress, and will spring rain offset summer drought (Mote et al. 2003)? Will longer growing seasons result in greater respiration than net primary production (NPP) and turn the PNW into a carbon source (Aber et al. 2001)? Will certain areas be vulnerable to carbon loss while others amenable to carbon gain? How will fire regimes respond to increases in precipitation variability and summer drought, and will the wet maritime forests that we think of as non-fire-prone burn (Littell et al. 2009)? As has been shown historically (Westerling et al. 2003), will the fire regimes of forests react more to drought while those of grasslands, shrublands, and woodlands react more to increases in precipitation? Will fire be the major driver of future ecosystem changes (Mote et al. 2003)? Generally, which ecosystems appear resilient to climate change, which appear vulnerable, and how quickly should we expect these changes (Climate Leadership Initiative 2008)?

Answers to these questions are important for various stakeholders. Multiple state (Tuttle and Andrasko 2005) and federal (Galik and Jackson 2009) policies are aimed at offsetting CO_2 emissions through afforestation and forest restoration and management. Knowledge of the spatial and temporal patterns of ecosystem vulnerability to carbon loss or gain under climate change is essential to these activities (Galik and Jackson 2009). Land and park managers concerned with storing carbon, protecting against high severity fires, and ensuring biodiversity must be aware of the influence of climate change on fire regimes and vegetation shifts (Mote et al. 2003, Climate Leadership Initiative 2008, Littell et al. 2009). Efforts to reduce high fuel loads from fire suppression must be targeted on vulnerable ecosystems (Littell et a. 2009, Blate et al. 2009). Running high-resolution (Diffenbaugh et al. 2003, Stephens et al. 2009) mechanistic ecosystem models (Scheller and Mladenorr 2007, Littell et al. 2009) under a range of future climate projections (Gavin et al. 2007, Climate Leadership Initiative 2008) is currently the best

method to address these questions under novel future climates and over large spatial and temporal domains.

We address these issues by running a dynamic general vegetation model, MC1, over much of the Pacific Northwest (PNW) at a high spatial resolution under nine future climate projections. We are interested in elucidating the drivers of vegetation, fire, and carbon stock changes, and how these vary by region within the PNW. In addition to the magnitudes of annual climatic changes, we consider the influence of changes in seasonality and summer drought, precipitation variability, fire and fire suppression, and CO_2 enrichment.

Methods

Study Area

Our study domain (Figure 1) spans the entire latitudinal expanse and roughly the western three-quarters of Oregon and Washington (41.9042° to 49.0042° latitude and -123.7370° to -118.7620° longitude). The longitudinal expanse was selected to represent the majority of climatic and ecosystem diversity within the region without unnecessarily increasing computing resource demands.

The domain was broken up by ecoregions (Bailey 1995) for analysis (Figure 1). To simplify the results, we aggregated ecoregions that experienced similar historical climates, displayed similar historical vegetation types, and reacted in comparable ways with respect to changes in vegetation, carbon, and fire under future climate projections. This resulted in three aggregated regions for analysis: the Western Forests (the Coast Range, Klamath Mountains, Willamette Valley, West Cascades, and North Cascades ecoregions), the Eastern Forests (the East Cascades, Okanagan, and Blue Mountains ecoregions), and the Columbia Plateau.

Because of the maritime influence, the Western Forests experience high rainfall and infrequent fires. The region therefore contains maritime forests with very high biomass. Summer drought causes occasional fires, but the return intervals are long. The Eastern Forests are considerably drier and experience larger seasonal temperature swings. There, precipitation is high enough to support forests, but fires are much more frequent. The Columbia Plateau is the driest of the three aggregated regions, and is dominated by shrubs, grasslands, and woodlands. Fires are frequent and can burn large areas, but consume relatively little biomass.

Input Data

MC1 requires inputs of gridded soils, monthly gridded climate, and yearly ambient CO_2 data. Soils data consist of bulk density, mineral depth, and three layers of sand, clay, and rock fragment fractions. The soils data were obtained from Kern (2000), using methodology from Kern (1995) with corrected inconsistencies and gap filling from NRCS (1994).

Monthly climate consists of precipitation, vapor pressure, mean temperature, and mean daily minimum and maximum temperatures. Historical climate data (1895–2006) were generated by the PRISM (Parameter-elevation Regressions on Independent Slopes Model) Climate Mapping Program at a 30-arc-second resolution (~ 649 x 926 m, or 0.6 km^2) and provided by the PRISM Group (Daly et al. 2008). For future climate (2007–2099), we used output from three general circulation models (GCMs) each run through three CO_2 emission scenarios. We selected output from the CSIRO Mk3 (Gordon et al. 2002), MIROC 3.2 medres (Hasumi and Emori 2004), and Hadley CM 3 (Johns et al. 2003) climate models (hereafter referred to as CSIRO, MIROC, and Hadley) run under the SRES B1, A1B, and A2 emission scenarios (IPCC 2000). The data were obtained from the World Climate Research Programme's Coupled Model Intercomparison Project phase 3 multi-model dataset (Meehl et al. 2007). The climate models were chosen for their range of temperature sensitivities. Globally, CSIRO displays low, MIROC high, and Hadley intermediate temperature sensitivities (Mote et al. 2008). Mote et al. (2008) compared historical output from 20 GCMs to NCEP/NCAR reanalysis data in the PNW, and found that CSIRO displayed low, MIROC displayed intermediate, and Hadley displayed high skill in reproducing yearly and seasonal climate variables. CO_2 emission scenarios were chosen for their range of total cumulative emissions by 2100. Of the chosen three, B1 contained the least, A1B contained intermediate, and A2 contained the highest cumulative emissions. The resulting three by three climate matrix was intended to span the broad range of possible futures. Annual atmospheric CO_2 concentrations were derived from the chosen SRES emission scenarios (Nakicenovic et al. 2000).

We used the delta, or perturbation, method to downscale future climate data (Fowler et al. 2007) to the 0.6 km^2 grid. More sophisticated downscaling techniques are available, such as statistical methods and regional climate models. However, the more complex statistical techniques add little skill over the delta method in producing monthly climatologies (Diaz-Nieto and Wilby 2005, Maurer and Hidalgo 2008), and regional climate models remain impractical for deriving century-long datasets of multiple climate scenarios (Fowler et al. 2007, Salathe Jr et al., 2007). For each variable, we calculated anomalies between the future and mean historical (1971–2000) GCM-simulated values. We used difference anomalies for temperature and ratio anomalies for vapor pressure and

precipitation (capped at maximum ratio of 5). These anomalies were then downscaled to our fine resolution grid using binomial interpolation and applied to mean historical climate from the PRISM model. To reduce GCM bias in temperature ranges, maximum and minimum temperature anomalies were calculated with respect to mean temperatures, normalized against historical ranges, and applied to future mean temperatures. Further details are given in Drapek et al. (2010, in prep).

We analyzed the domain-averaged inter-annual and inter-decadal variability of historical and future precipitation. Because of its effects on production, respiration, fuel moisture, and conditions for ignition, precipitation variability exerts a strong control on ecosystem dynamics, especially fire behavior (Hessl et al. 2008). We calculated inter-annual variability in precipitation by the following equation:

$$\sigma_i = \sqrt{\frac{\sum_{j=2}^{n}(Y_j - Y_{j-1})^2}{n-2}} \quad (1)$$

where σ_i = inter-annual variability, n = number of years, and Y_j = the precipitation for year j. This formula is similar to standard deviation, but calculated relative to the previous year's observation. We analyzed inter-decadal precipitation variability in three ways. First we used r_1, the correlation of consecutive residuals, defined by the following equation:

$$r_1 = \frac{\sum_{j=2}^{n}\left(res_j \times res_{j-1}\right)}{\sum_{j=1}^{n} res_j^{\,2}} \quad (2)$$

where n = number of years and res_j = the residual between year j's precipitation and that predicted by a linear regression model fit to the time series. r_1 provides the strength of correlations between adjacent residuals, and will be higher in time series that display long-term runs above and below a regression line. We also used a non-parametric runs test to assess inter-decadal precipitation variability. Resultant negative Z-values signify time series that display a fewer than expected number of runs below or above the regression line, and therefore inter-decadal variability. We based all calculations on 93

years of precipitation data (2007–2099 for future and 1914–2006 for historical). We also performed Fast Fourier Transforms (FFTs) on the precipitation time series and analyzed the power distributions. FFTs measure the power of underlying frequencies in a time series: years with a higher power denote a more influential frequency in the time series oscillations.

Model

MAPSS-CENTURY 1 (MC1) is a dynamic general vegetation model that originated from a coupling between the MAPSS biogeography model (Neilson 1995), the CENTURY biogeochemistry model (Parton et al. 1994), and MCFIRE, a mechanistic fire model (Lenihan et al. 1998). MC1 simulates lifeform mixtures and resulting vegetation types, wildfire, and ecosystem fluxes of carbon, nitrogen, and water. The model is routinely implemented on time scales of months to centuries. MC1 is one-dimensional, and can therefore be implemented on any spatial scale without fundamental changes to its parameterizations. Typically, however, it us run on scales from 50 meters to 0.5° latitude/longitude. MC1 reads monthly climate data and calls interacting biogeography, biogeochemistry, and fire disturbance modules.

Biogeography Module

The biogeography module acts as a lifeform interpreter that parameterizes the biogeochemistry and fire modules. It is based on the philosophy that, after accounting for nutrient constraints, plants will maximize leaf area during the growing season to just use up the available soil water. The module uses tree and grass carbon pools from the biogeochemistry module and climatic indices to assign one of 35 vegetation types to a grid-cell each year. A grid-cell is designated as grassland only if grass carbon is above a minimum threshold (113 g C m^{-2}) and tree carbon is below another (300 g C m^{-2}). Shrubs are simulated as small-stature trees. Thresholds of woody carbon density delineate forests from woodlands and shrublands.

Tree lifeform dominance is determined by locating the grid-cell on a two-dimensional array of annual minimum temperature and growing season precipitation. Evergreen needle-leave trees are dominant at the cold end of the temperature spectrum (-

15°C) and evergreen broadleaf trees are dominant at the warm end (18°C). Deciduous broadleaf trees are dominant at the midpoint of the spectrum, and growing season precipitation modulates their relative proportion. The relative proportion of C3 and C4 grasses is based on the potential growing season productivity of each grass type.

After the proportion of relevant lifeforms is determined, the module uses climatic indices to assign vegetation types. For example, temperature thresholds are used to distinguish subalpine from temperate and subtropical coniferous forests. Of the possible 35 vegetation types, 11 occur in the historical PNW simulation, and 12 occur in future simulations. Regional examples of the simulated vegetation types are given in Table 1.

Biogeochemistry Module

The biogeochemistry module simulates water and nutrient cycling, plant productivity and mortality, and organic matter decomposition. Lifeform types from the biogeography module are used to parameterize numerous biogeochemistry functions, and fires simulated by the fire module impact numerous live and dead carbon and nutrient pools. Nitrogen is transferred between carbon pools and is constrained by maximum and minimum C:N ratios. Plant-available nitrogen is lost through denitrification and volatilization, gained through biotic and abiotic fixation, and recycled through mineralization. As of yet, MC1 does not consider anthropogenic nitrogen deposition or potential changes in carbon and nitrogen coupling in future climates, which may have large effects on the carbon balance (Thornton et al. 2009).

The biogeochemistry module's hydrologic functions affect most processes in MC1. Potential evapotranspiration (PET) is calculated with equations from Linacre (1977), modified by Monteith (1995). Canopy interception and bare soil evaporation are functions of aboveground biomass, precipitation, and PET. Water percolates downward through soil layers as saturated flow above field capacity, which is a function of bulk density, soil texture, and organic matter. Both grasses and trees can access water in the upper soil layers, but only trees can access water from the lower layers. Water stress is defined as:

$$\text{water stress} = 100 * \left(1 - \frac{w_s}{PET}\right) \quad (3)$$

where w_s = mean monthly available soil water, weighted by root distributions, and PET = potential evapotranspiration, both in cm month^{-1}.

Tree and grass productivity are constrained by temperature and competition for available soil water, nutrients, and light. Increases in tree biomass reduce the light available for grass productivity. Grass production is allocated to leaf and fine root pools, and tree production is allocated to leaf, fine branch, large wood, coarse roots, and fine roots. Mortality is simulated by the transfer of live biomass to dead belowground and aboveground litter pools. Increasing atmospheric CO_2 increases maximum potential productivity and decreases the moisture constraint on productivity by increasing water use efficiency. For our control runs, we used a logarithmic biotic growth factor (β-factor) (Wullschleger et al. 1995, Amthor and Koch 1995) of 0.25 for the increase in net primary production (NPP) and decrease in transpiration associated with increases in atmospheric CO_2 above 350 ppm, although this was varied in sensitivity analyses.

Fire Module

The fire module simulates the occurrence, intensity, and effects of fire. It receives information on vegetation type from the biogeography module and carbon pools from the biogeochemistry module. The fire module distinguishes two live and four dead fuel classes. Fuel moisture content is affected by antecedent climatic conditions and, in the case of live fuels, by soil moisture. Ignition is assumed once the largest dead fuel class and rate of spread exceed certain thresholds. A grid-cell's burn area is calculated from the time since previous fire and potential rate of spread. Vegetation consumed within a burned area is a function of fire type and intensity.

We developed a new optional fire suppression rule for this study based on the philosophy that 95% of historical fires in the western U.S. have been suppressed since 1940, and that the remaining 2-5% of un-suppressed fires burn approximately 95% of the area (Graham et al. 1999). To emulate this, fires associated with a calculated fireline intensity above a given threshold were allowed to burn naturally. Below this threshold, burn area was capped at 0.06% of the grid-cell per fire. While this rule cannot capture many of the subtleties and idiosyncrasies of 20th century fire suppression, it resulted in

accurate historical burn areas in the PNW and may better simulate some of the effects of fire suppression on ecosystem structure and function.

Calibration and Validation

MC1 was calibrated and validated against a variety of observational datasets. We corrected model inconsistencies and tuned fire behavior, death rates, and biogeography thresholds to more accurately simulate vegetation, fire, and carbon dynamics in the PNW (Appendix A).

Simulated modal vegetation types for the period 1971-2000 were calibrated against a potential vegetation map from Kuchler (1975), in which vegetation types were aggregated into 35 classes as part of the VEMAP project (Vegetation/Ecosystem Modeling and Analysis Project, Kittel et al. 1995). Modeled fire behavior is difficult to calibrate directly because of the lack of fine-resolution gridded data and the human influence via fire suppression and management over the 20th century (Agee 1993). However, we were able to compare means and temporal patterns of simulated burn area from 1980-2004 to a 1° x 1° grid of observed annual burn area derived from Westerling et al. (2003), both for control runs and for developing the new fire suppression rule. We also compared simulated combustion factors (fraction of pre-burn mass lost to combustion in fire) from 2002 in the Klamath Mountains ecoregion with data from Campbell et al. (2007) on the 2002 Biscuit fire of southwest Oregon. Combustion factors from individual carbon pools were combined using mass weighting factors from both Campbell et al. (2007) and MC1.

Carbon fluxes and pools were compared against four datasets. We used an aggregated database of periodic Forest Inventory and Analysis (FIA) plots in Oregon from Hudiburg et al. (2009) to calibrate NPP, mortality, and live and dead aboveground and belowground carbon pools. We ran MC1 under varying conditions, including full fire, fire suppression, and no fire, to emulate plots classified by ecoregion and disturbance history. We then used an interpolated map of aboveground forest biomass from Blackard et al. (2008), which used FIA plots and MODIS satellite data, to validate ecoregion-specific aboveground forest carbon over the entire domain. A separate calibration was carried out using data on old-growth forests in the Western Forests region from three

datasets: Smithwick et al. (2002), periodic FIA plots from Hudiburg et al. (2009), and plots from the ORCA regional carbon study (DOE and Environmental Protection Agency (EPA)) from Campbell et al. (2007) and Hudiburg et al. (2009). To ensure simulated grid-cells were undisturbed, we ran MC1 without fire. Old-growth forests were defined as those older than 180 years according to the Spies and Franklin or Van Tuyl method (Spies and Franklin 1991, Van Tuyl et al. 2005). We only analyzed old-growth forests in the Western Forests region because of the difficulties and inaccuracies involved in prescribing the disturbance histories of old-growth forests in the Eastern Forests region. The majority of all plot data were collected between 1991-2001, with a few observations post-2001. We therefore used MC1 annual average output from 1991-2001. We also compared the seasonality of NPP against eddy covariance data from the Metolius Intermediate Pine site (US-Me2, Law et al. 2003) and the MODIS Aqua satellite product (Running et al. 2004). Flux data were available from 2002–2007 with missing values in 2003, and MODIS data were available from 2003–2007. In all plot-based comparisons, MC1 output was extracted from the grid-cell containing the location of a given observational plot. Appendix A contains all the associated code and parameter changes.

Model Runs

We first ran MC1 under an average monthly climate derived from 1895-2006 means to establish vegetation types and build carbon and nutrient pools. This step proceeded with prescribed fires based on vegetation type for up to 3,000 simulation years until the recalcitrant soil carbon pool approached equilibrium. We subsequently ran MC1 with dynamic fire under a "spinup" climate derived from a de-trended and looped 1895-2006 time series. In past studies this step was conducted for 500 simulation years, but we extended it to 3,000 years to accommodate the slow buildup of carbon in the high-biomass forests of western OR and WA that rarely burn. Finally, MC1 was run through the historical climate from 1895–2006, and then the future climates from 2007–2099. Soils were held constant in all model runs. MC1 contains the option of using fire suppression, turning fire off, and turning nitrogen limitation off. Aside from calibration and sensitivity analyses, we ran MC1 with its fully functional fire module, nitrogen limitation, and a CO_2 enrichment β-factor of 0.25. These conditions define our control

runs. In the following analyses, unless otherwise noted, historical values refer to means between 1971-2000 and future values refer to means between 2070-2099. Changes refer to differences between the two time periods.

We conducted a number of sensitivity analyses to assess the modeled influences of fires, fire suppression, CO_2 enrichment, and precipitation variability on carbon and fire variables. Except for the precipitation variability sensitivity runs, all sensitivity analysis simulations were run through the historical period and then under projected future climates derived from the three GCMS run under the A2 emissions scenario. The A2 emissions scenario, which we are currently surpassing (Raupach et al. 2007), contains the highest cumulative emissions by 2100 of our three scenarios. We ran MC1 with full fire, fire suppression, and no fire in order to assess the modeled influence of fire suppression on future fires, and the influence of future fires on the carbon balance. When calculating changes, we referenced future runs against historical simulations with the same fire prescription. We also assessed the model's sensitivity to the logarithmic β-factor by running MC1 with a β-factor of 0.0 (no CO_2 enrichment affect) and 0.6 (greater CO_2 enrichment affect) instead of the control value of 0.25. Norby et al. (2005) report a β-factor of 0.6 for experimental FACE sites, but recent results show NPP enhancement may decrease by 50% or more due to water and/or nitrogen limitations (Norby et al. 2008). To assess the impact of precipitation variability on fire behavior, we placed a three and a five-year filter on precipitation values from the CSIRO A2 climate. This preserved seasonality patterns and long-term annual precipitation means, but significantly damped the inter-annual variability.

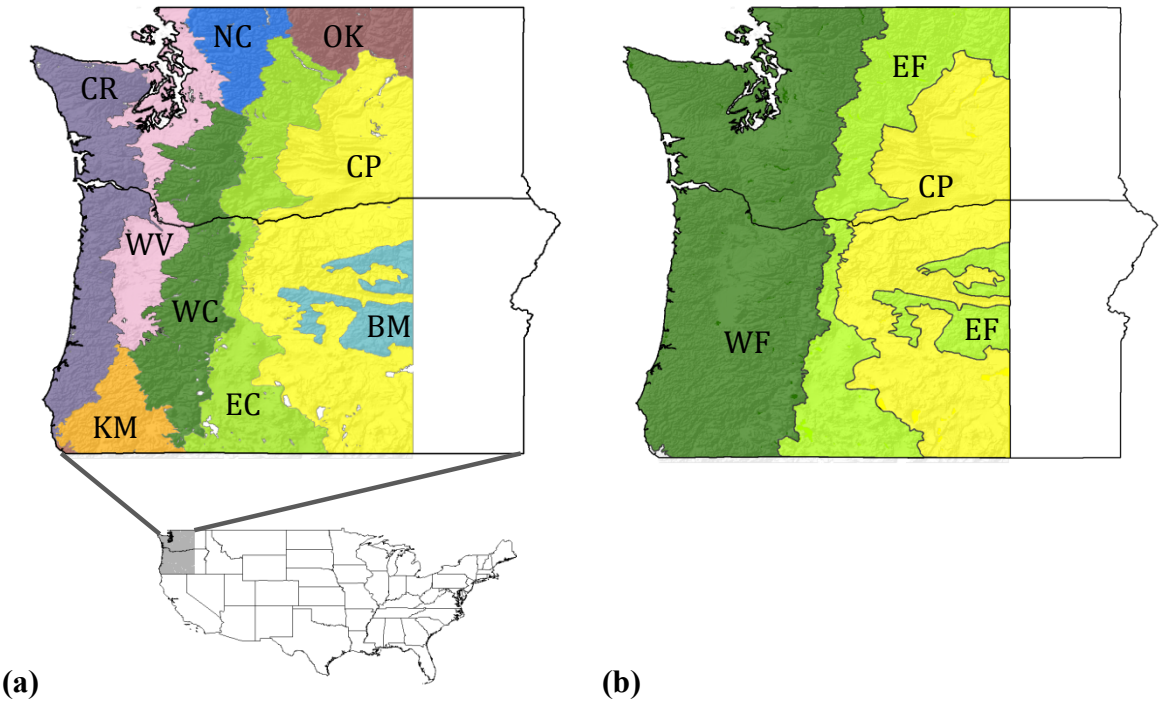

Fig 1. Study area. (a) Ecoregions: BM = Blue Mountains, CP = Columbia Plateau/Northern Basin, CR = Coast Range, EC = East Cascades, KM = Klamath Mountains, NC = North Cascades, OK = Okanagan, WC = West Cascades, WV = Willamette Valley/Puget Trough. (b) Aggregated regions: CP = Columbia Plateau, EF = Eastern Forests, WF = Western Forests.

Table 1. Regional examples of MC1 vegetation types

MC1 vegetation type	Regional examples
Ice	Barren Rock, Permanent Snowpack
Tundra	Alpine Meadows
Subalpine Forest	Subalpine Fir, Lodgepole Pine, Mountain Hemlock, Whitebark Pine Forest
Maritime Conifer Forest	Douglas Fir, Western Hemlock, Sitka Spruce, Pacific Silver Fir Forest
Temperate Conifer Forest	Ponderosa Pine, Douglas Fir, Lodgepole Pine, Grand Fir, White Fir, Western Juniper Forest
Temperate Cool Mixed Forest	Douglas Fir-Garry Oak Forest
Temperate Warm Mixed Forest	Douglas Fir-Garry Oak-Madrone Forest
Temperate Deciduous Broadleaf Forest	Oregon White Oak, Bigleaf Maple Forests
Temperate Conifer Woodland	Ponderosa Pine-Western Juniper Woodland
Temperate Shrubland	Big Sagebrush-Bluebunch wheatgrass Big Sagebrush-Idaho Fescue
Temperate Grassland	Idaho Fescue Bluebunch Wheatgrass
Subtropical Mixed Forest	Douglas Fir-Madrone-Tanoak Forest

Results

Historical

Although the study area includes coastal forests, valleys, high-elevation mountains, and dry steppes, there were consistent historical seasonal climatic patterns. Precipitation was highest in winter and lowest in summer while temperatures displayed the opposite trend (Figure 2). Because of these patterns, the region experienced substantial simulated water stress in late summer, but little during the winter and spring. Simulated net primary production (NPP) showed peaks in late spring and fall, when available soil water was relatively high and temperatures were warm (Figure 2). Low temperatures limited production in winter while drought stress limited production in summer.

Under the influence of historical climate, MC1 simulated the expected distributions of carbon stocks, fire, and vegetation types (Figures 3 and 4). MC1 simulated the Western Forests region as containing high-biomass maritime forests with infrequent fires (except in parts of the Klamath Mountains). The Eastern Forests contained mostly temperate coniferous forests with large amounts of biomass combusted. MC1 simulated mixes of woodlands, shrublands, and grasslands in the Columbia Plateau that burn frequently at low intensities.

Simulated modal (most frequent) vegetation types during 1971-2000 compared well with those from Kuchler (1975) (Figures 4 and 5). Disagreements between the two occurred mainly in the Willamette Valley and exterior edges of the Columbia Plateau. In the Willamette valley, Kuchler's potential vegetation map showed a large expanse of temperate cool mixed forests (mixed oak forests), whereas MC1 simulated only maritime conifer forests. The Kuchler map displayed continuous expanses of grasslands in parts of the northern Columbia Plateau, whereas MC1 simulated a patchwork of grasslands bordering the region's exterior. However, Native Americans and European settlers greatly modified the fire regime in the Willamette Valley (Whitlock and Knox 2002), thus allowing the establishment and maintenance of mixed oak forests and woodlands. Additionally, the Columbia Plateau is particularly sensitive to both grass (Keane et al. 2008) and woodland (Belsky 1996) encroachment. These facts may complicate the assignment of potential vegetation communities within the two regions.

Simulated carbon pools and fluxes compared relatively well with the FIA-derived database from Hudiburg et al. (2009) (Figures 6 and 7). Although MC1 simulated consistently higher values for carbon pools and fluxes than did the FIA plots ($p < 0.001$ in all pools and fluxes), the FIA data include sites influenced by both natural and anthropogenic disturbances (Van Tuyl et al. 2005). MC1, however, only accounts for natural fire disturbance. Many areas within the Western Forests, particularly the Coast Range, Willamette Valley, and to some extent the West Cascades ecoregions, were subject to heavy human influence during the 20th century, including land conversion, logging, and urbanization. Figure 8 shows average harvest values over the domain. These human impacts all acted to decrease total ecosystem carbon (Smithwick et al. 2002). Figure 7 shows that MC1 was unable to capture the distribution of observed total live carbon in the Western Forests, primarily because it does not account for these human influences. In the Eastern Forests and Columbia Plateau regions, 20th century fire suppression has increased woody carbon and total carbon stocks (Agee 1993). Consistent with this, MC1 simulated higher than observed live aboveground forest carbon in the Western Forests, but lower than observed values in the Eastern Forests and Columbia Plateau when compared with data from Blackard et al. (2008) ($p < 0.001$ in all three cases, Figure 9).

Comparisons of old-growth stands between MC1 (run without fire) and observations in the Western Forests produced mixed results (Figure 10). MC1 simulated significantly higher live carbon values in old-growth forests than periodic FIA plots from Hudiburg et al. (2009) ($p < 0.001$). Conversely, MC1 simulated significantly lower live carbon values than EPA plots from Hudiburg et al. (2009) ($p < 0.01$), and significantly lower live, dead, and total ecosystem carbon than plots from Smithwick et al. (2002) ($p < 0.001$ for all pools). These discrepancies may be due to differing methods of plot selection in the above studies (Van Tuyl et al. 2005).

The overall seasonal patterns of NPP were comparable between MC1 and observations, but there were notable differences. Compared with the Metolius eddy covariance data from the East Cascades, MC1 simulated a deeper and longer drop in NPP during late summer months, and increased winter NPP (Figure 11). Figure 12 shows these same discrepancies between MC1 and MODIS Aqua satellite data over large spatial

extents. In all three aggregated regions, MC1 simulated deeper and lengthened late summer NPP drops, later and larger fall NPP boosts, and elevated winter NPP values. These biases may carry important implications for the simulated responses under future climates.

Without fire suppression, MC1 simulated about eight times more burn area during 1980-2004 than Westerling et al. (2003) reported for the region. This is consistent with previous MC1 studies over the continental U.S., which showed an over-simulation of burn area by a factor of about eight since 1960. Before 1960, MC1 accurately simulated continental annual burn area (Neilson 2004). The new fire suppression rule was calibrated to this Westerling data, and over-estimates 1980-2004 burn area by 1.3%. Figure 13 displays time series for domain-averaged observed and MC1 simulated burn area. Although simulated fire suppression cannot account for all the idiosyncrasies and local differences in actual suppression and ignition, MC1 captures the overall historical temporal patterns well. MC1 displayed a slight over-estimation of combustion factors compared with data from Campbell et al. (2007) (Figure 14). However, MC1 is designed to simulate large fires, as these contribute over 95% of the annual burn area in the U.S. (Graham et al. 1999).

Future Climates

Future climate projections came from a three by three matrix defined by GCMs and CO_2 emission scenarios. Although domain-averaged temperatures increased concurrently with increasingly higher emission scenarios (B1 < A1B < A2, Table 2), GCMs explained more variability than did emission scenarios (p-values of 0.015 and 0.0015 vs. 0.63 and 0.014 in two-way ANOVA of changes in precipitation and mean temperature, respectively). This became even more apparent after assessing spatial and temporal patterns of climate and model output. Many of the results were therefore aggregated by GCM for analysis and discussion. Future maps and time series display results under the A2 climate projections, as we are currently surpassing this emission scenario (Raupach et al. 2007), the highest of our three.

CSIRO climate projections were generally the coolest and wettest of the future scenarios (Table 2). Domain-wide projected precipitation was greater than historical

throughout the fall and winter, but remained similar to historical in the spring and summer months (Figure 15(a)). CSIRO temperature increases were relatively uniform throughout the year, although slightly higher in summer and early fall (Figure 15(b)). MIROC projections were consistently wet and hot (Table 2). However, the seasonality of precipitation was stronger. MIROC precipitation was generally somewhat less than historical in spring and summer, but showed large increases in the late fall and early winter (Figure 15(a)). Like CSIRO, MIROC temperature increases were slightly higher in the summer and early fall. Hadley projections, on the other hand, were decidedly hot and dry (Table 2). Through the winter months, Hadley precipitation was similar to historical. Yet it was considerably drier in spring and summer (Figure 15(a)). Hadley temperature increases were relatively modest in the winter, but showed large spikes in summer and early fall that well surpassed MIROC temperatures and approached 8°C (Figure 15(b)). Hadley vapor pressure deficits (VPDs) were nearly twice as high as historical in summer months: mean VPD during June, July, and August was 888 Pa during 1971-2000, and 1,565 Pa during 2070-2099 under Hadley projections. Our projected changes in the seasonality of climatic variables agree qualitatively with those from Mote et al. (2008). Appendix B contains yearly climatic variables for all climate scenarios and all regions.

Inter-annual variability in precipitation increased for all CSIRO and MIROC climate projections, and decreased for all Hadley projections (Table 3). CSIRO consistently displayed the largest increases. Inter-decadal variability, measured by both r_1 and runs tests, was less than historical for all future projections. The only climate scenario with a significant runs test was historical. Figure 16 shows the power spectrum from the Fast Fourier Transforms (FFTs). The historical time series displays peaks in the 3-5 year range, and again in the 8-9 year range. These peaks are notably different in future scenarios. In nearly all cases, the 1-2 year peaks are significantly higher. This signifies higher-frequency oscillations of precipitation, indicative of higher inter-annual variability. Future climates that still display signs of inter-decadal variability (relatively high r_1's and negative Z_{runs}-values), such as CSIRO A1B and MIROC A2, also display higher FFT peaks in the 8-9 year range. Other climates have very large 1-2 year signals and/or decidedly dampened 8-9 year signals, and therefore display little to no noticeable inter-decadal variability. These differences in variability may be due to GCM-simulated

trends or, consequently, inherent GCM inaccuracies. Because we did not downscale historical GCM data, we were unable to determine the origin.

Future Model Output

MC1 simulated substantial changes in future vegetation distributions (Figures 17 and 18). Because of increases in temperatures and growing-degree days, most of the region's tundra and subalpine forests were lost. Figure 19 shows that changes in mean subalpine forest ecotone elevations were a linear function of mean annual temperature increases. In the Western Forests region, higher minimum winter temperatures decreased the frequencies of frosts and allowed for the expansion of subtropical and warm mixed forests. In MC1, subtropical forests predominate in areas where the mean daily minimum temperature during the coldest month is above 7.5 °C. Large areas of shrublands were converted to grasslands in the northern Columbia Plateau, and into both grasslands and woodlands in the southern Columbia Plateau. CSIRO projections showed the largest conversion of shrublands. Because of its high winter temperatures, MIROC showed the largest expansions of subtropical forests. With its large increases in the range of seasonal temperatures, Hadley climates produced large conversions of maritime conifer forests into temperate conifer forests in the Western Forests. In MC1, maritime forests predominate in areas where the range of monthly mean temperatures is less than 18 °C. One should note that although there are modeled time lags with the above conversions between forest types, these differences are based purely on climatic indices.

Future climate projections increased the seasonal amplitudes of NPP and water stress (Figure 15(c,d)). Because of elevated precipitation and temperatures, simulations under CSIRO projections showed increased NPP and decreased water stress through the fall, winter, and spring months. Only in late summer was there a noticeable increase in water stress and resultant decrease in NPP. MIROC climates displayed the largest increases in both fall and winter precipitation and temperatures. This led to the highest NPP values in fall and winter. However, simulations under MIROC climates experienced significantly elevated water stress in spring and summer months that led to decreased NPP. Hadley runs showed increased fall, winter, and spring NPP similar to CSIRO, but severely decreased NPP and increased water stress in the late spring and summer months.

The seasonal changes in NPP and water stress have the potential to be exaggerated in MC1 because of the model's apparent bias towards lower summer and higher winter NPP values compared against observations.

These changes in the seasonal amplitudes of NPP and water stress produced pronounced changes in fire behavior and carbon stocks. Across the entire domain, burn area and biomass lost to fire increased substantially under all future scenarios (Table 4). CSIRO climates resulted in significantly more fire than did MIROC, despite the fact that MIROC warmed more. Hadley climates resulted in extreme increases of biomass combusted. The large increases in wildland fires under Hadley and CSIRO are tightly coupled with carbon losses (Figure 20). We found strong negative spatial correlation coefficients between biomass lost to fire and changes in ecosystem carbon for Hadley and CSIRO, but not for MIROC scenarios (Table 5). With their large fires, Hadley climates produced nearly 15% losses in total ecosystem carbon (1,256 Tg) and 37% losses in live vegetation carbon (1,568 Tg) across the entire domain (Table 4 and Appendix C). CSIRO scenarios lost an average of 1.2% (104 Tg), and MIROC scenarios gained an average of 0.8% (72 Tg) ecosystem carbon.

In all scenarios, carbon stocks declined during the second half of the 21st century (Figure 21). Carbon losses were entirely from live vegetation: total dead carbon (including soil organic matter) increased ubiquitously (Appendix C) because of drought-related death and increased fires. Although litter and dead fuels were burnt in the more frequent future fires, forest biomass killed but not combusted caused the increases in dead carbon pools. Spatial patterns of fire and carbon changes were nearly identical within a given GCM across emission scenarios (Appendices E, F, and G). Estimates of biomass combusted and subsequent carbon loss may be somewhat overestimated in MC1 because of its slight overestimation of combustion factors compared with Campbell et al. (2007).

The Western Forests region displayed the largest increases in fire effects and decreases in carbon stocks (Table 4). Runs under Hadley climates were the most extreme, and averaged 13-fold increases in biomass combusted, 7-fold increases in burn area, 18% decreases in ecosystem carbon, and 41% decreases in live vegetation carbon. While less extreme, CSIRO climates burned over three times more carbon than historical. Fire intensities, measured by biomass combusted per unit burn area, increased in the region

under all future scenarios. Particular areas within the Western Forests, such as the greater Klamath Mountains and western North Cascades, appear particularly vulnerable to increases in fire behavior and decreases in carbon stocks (Figure 20). Others, such as the Olympics and Cascade crest, appear relatively resilient.

Net ecosystem production (NEP, NEP = NPP – heterotrophic respiration) can be used as an effective barometer of an ecosystem's carbon balance. In MC1, NPP is more sensitive to environmental conditions than heterotrophic respiration. Therefore, conditions that increase NPP, such as increased winter temperatures and precipitation, also increase NEP. Conditions that decrease NPP, such as increased summer water stress, decrease NEP. NEP is also strongly negatively affected by fires, which decrease leaf area and thus NPP but increase dead carbon to be respired.

Figure 22 shows time series of biomass consumed by fire, NEP, and total ecosystem carbon for the A2 scenarios averaged across the Western Forests. Runs under CSIRO A2 displayed a mildly increased fire regime from 2035-2070, and substantially elevated regime from 2070-2099, which negatively affected NEP and carbon stocks. Although runs under MIROC A2 showed increases in fire occurrence towards the very end of the 21st century, carbon loss was a result of fire-independent decreases in NEP until then. Under Hadley A2, NEP and carbon stocks in the Western Forests displayed strong negative responses to a highly elevated fire regime beginning relatively early in the century. Figure 23 shows results from a representative grid-cell in the West Cascades under the A2 scenarios. Under CSIRO A2, positive NEP raised ecosystem carbon until two large fires in the last quarter of the 21st century decreased stocks. Under MIROC A2, carbon stocks increased until mid-century when negative NEP values caused a decrease. One large fire was simulated in 2099 and carbon dropped significantly. Hadley A2 showed an entirely different fire regime beginning in the 2020s, characterized by more frequent but less intense burning. Vegetation carbon was reduced by 33% by the end of the century, but appeared to approach equilibrium. We should note that model biases towards decreased summer NPP could indicate an exaggerated sensitivity to summer drought, and this could in turn amplify future responses in fire regimes.

The Eastern Forests region is drier and historically experienced much more fire than the Western Forests. Since it was already adapted to a more frequent fire regime, it

was less vulnerable to future climates in MC1. While fire increased ubiquitously, fire intensities decreased. The region only lost carbon under Hadley climates, and these losses were modest (Table 4). There were also very few changes in vegetation distributions in the Eastern Forests. Fire behavior tended to increase, and carbon stocks decrease, on the northern and western reaches (Figure 20). Conversely, the eastern and southern sub-regions appear resilient to change, and fires even decrease over a relatively large expanse of the southern East Cascades.

Figure 22 shows that changes in fire regimes had a smaller influence on the region-wide carbon balance here versus the Western Forests. In CSIRO A2, biomass lost to fire steadily increased throughout the 21st century, but so did NEP and consequently ecosystem carbon. Under MIROC A2, NEP steadily increased until 2065, when fire occurrence increased and NEP decreased. Live vegetation carbon declined, but dead carbon increased due to fire mortality (not shown), and total carbon therefore stabilized. Under Hadley A2, NEP stayed relatively stable but biomass lost to fire quickly reached and maintained an elevated level. Ecosystem carbon therefore steadily declined but the curve's concavity suggests equilibrium would be reached soon after 2100. The increases in NEP can be attributed to increases in fall and winter temperatures and precipitation, and therefore NPP, in the Eastern Forests: CSIRO models averaged 105%, MIROC averaged 149%, and Hadley averaged 102% increases in NPP in the fall and winter months.

Changes in the Columbia Plateau were closely associated with increases in precipitation. Converted shrubland area and changes in biomass consumed by fire, burn area, and ecosystem carbon all followed trends in annual precipitation (Hadley < MIROC < CSIRO, $p < 0.001$ for all variables regressed on changes in annual precipitation for nine projections). Grass and consequently fine fuel production increased, and much of the area therefore experienced increased fires and transitions to grasslands. However, tree production also increased and woodlands appeared in areas where woody vegetation survived fires and could out-compete grasses for available soil water. Because the woodlands sequestered more carbon than was lost by conversion to grassland, the region gained carbon in all scenarios. Fire intensities decreased because of the relative increases in grassland fires. The Columbia Plateau's interior appeared relatively resilient to

changes, while the exterior appeared vulnerable to increased fires and grassland conversion.

Figure 24 depicts the two shrubland conversion pathways in the Columbia Plateau and their driving factors. Shown is the simulation of two representative and adjacent grid-cells under CSIRO A2 with near-identical historical conditions. Both were historically shrubland, yet one became a stable grassland and the other a stable woodland. The first grid-cell experienced large fires between 2017 and 2023. Thereafter, the cell transitioned to a state with increased grass carbon, decreased woody carbon, and an elevated fire regime. Large fires, however, were not simulated early in the 21st century in the second grid-cell. Here, woody vegetation continued to increase in biomass and out-compete grasses. The fire regime was not strong enough to kill the woody vegetation. Shrubland conversions followed similar trajectories across the region and under different future climate projections.

Our fire-based sensitivity analyses revealed the modeled impact of fire suppression on future fires, and the influence of future fires on carbon stocks (Table 6). Compared to control runs, fire suppression runs produced increased future carbon storage. However, they also produced greater absolute and percentage increases in biomass lost to fire (calculated against historical fire suppression runs), and greater percentage increases in area burned than control runs. These relative increases in future fire under fire suppression were concentrated in the Eastern Forests and Columbia Plateau: from control to fire suppression runs, increases in biomass combusted went from 639% to 652% in the Western Forests, from 34% to 105% in the Eastern Forests, and from 16% to 438% in the Columbia Plateau. Without any fire, the domain gained carbon under all A2 scenarios. However, carbon stocks under MIROC A2 and Hadley A2 projections show a downward trend after about 2070 (Figure 25), as in the control runs. Together, these fire sensitivity analyses suggest that the utility of fire suppression may decline, that fire is a major driver in the region's future carbon budget, and that because of worsening summer drought and decreasing NEP, the PNW may be a carbon source even in the absence of fires during the last 30 years of the 21st century.

MC1 displayed a minimal sensitivity to changes in the CO_2 enrichment β-factor, but a high sensitivity to precipitation variability (Table 6). Compared to control runs,

increased β runs produced slightly higher carbon storage and burn areas, and slightly less biomass combusted. Decreased β runs displayed the opposite trends. With an increasing β-factor, the Western and Eastern Forests regions burn less whereas the Columbia Plateau burns more: between a β-factor of 0.0 and 0.6, increases in biomass combusted went from 644% to 618% in the Western Forests, from 35% to 30% in the Eastern Forests, and from 13% to 20% in the Columbia Plateau, averaged across all future scenarios. These regional differences reflect the varying limitations on fire. With an increasing β-factor, water use efficiency and NPP increase. This decreases fires in the forested regions because it alleviates summer drought. Yet a higher β-factor increases fires in the Columbia Plateau because it increases winter and spring fuel production but does little to alleviate the hot and dry summers that spark fires.

By applying three and five-year filters on CSIRO A2 precipitation, we preserved monthly and seasonal means but considerably dampened variability (σ_i = 6.73 and 4.24 for the three and five-year filters, respectively, versus 19.93 for control). In response to this, MC1 simulated carbon gains instead of losses under CSIRO A2, and changes in biomass lost to fire decreased from 15.0 g C m^{-2} yr^{-1} in the control run to 9.8 and 7.7 g C m^{-2} yr^{-1} under the three and five-year filters, respectively. These biomass combusted values bracket that of the MIROC A2 control run. These decreases in fire behavior occurred almost exclusively in the Western Forests. Biomass combusted increased by 366% in the control CSIRO A2 run, whereas it only increased by 209% and 164% in the three- and five-year filter runs, respectively. Conversely, biomass combusted increased by 31%, 27%, and 20% in the Eastern Forests, and by 26%, 25%, and 23% in the Columbia Plateau, under the control, three-year, and five-year filter runs, respectively.

Uncertainties

This study contains four major sources of uncertainties: our chosen (1) CO_2 emissions scenarios, our selected (2) GCMs, (3) our downscaling process, and (3) our dynamic general vegetation model, MC1. Both the IPCC (IPCC 2007) and our study assign equal probabilities to CO_2 emission scenarios, and this may be misleading. Currently we are surpassing the highest emission scenario, A1F1 (Raupach et al. 2007). GCMs display wide ranges of climatic responses to increasing atmospheric CO_2, both

globally and in the PNW (Mote et al. 2008). Our selection of three emission scenarios and three GCMs was meant to address these two uncertainties. Our chosen method of downscaling, the delta method, contains major assumptions. Among them, the method assumes that GCM biases will remain constant in the future, that these biases are fully described by climatic means, and that anomalies are spatially conserved. Finally, MC1 contains many sources of uncertainty. MC1 considers no anthropogenic effects except atmospheric CO_2 and climate change. There is no grid-cell communication, which may be important for hydrology, fire behavior, and vegetation migrations. We have also discovered a strong bias in the seasonality of NPP that may render MC1 too sensitive to future changes in summer drought, which may affect estimates of vulnerability to fire and vegetation shifts. Part of this may be due to an over-dependency on rain-related nitrogen fixation, and part may be due to not accounting for the effect of low sun angle on NPP. Accounting for this would reduce the effect of increased future precipitation on NPP in the fall, winter, and spring months (Landsberg and Waring 1997), and potentially dampen the simulated effects of increased summer drought.

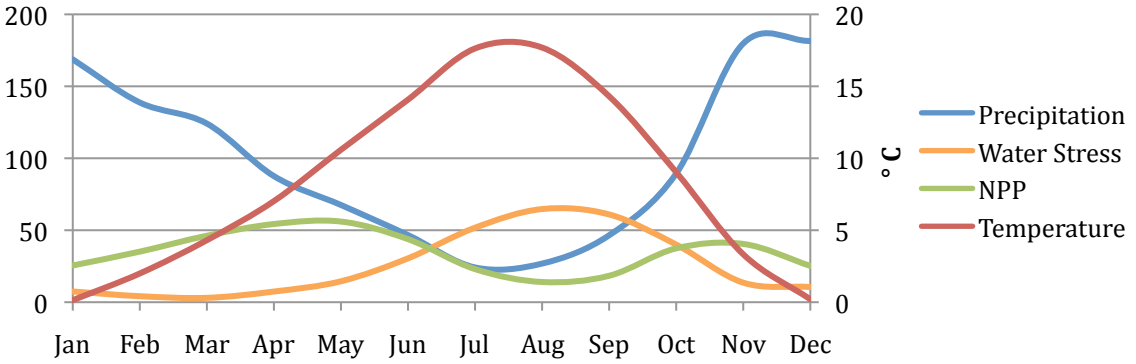

Fig 2. Seasonality of mean historical temperature (°C, right-hand axis), precipitation (mm H_2O $month^{-1}$, left-hand axis), MC1 simulated NPP (g C m^{-2} $month^{-1}$, left-hand axis) and water stress (unitless, left-hand axis, equation 2) over entire domain.

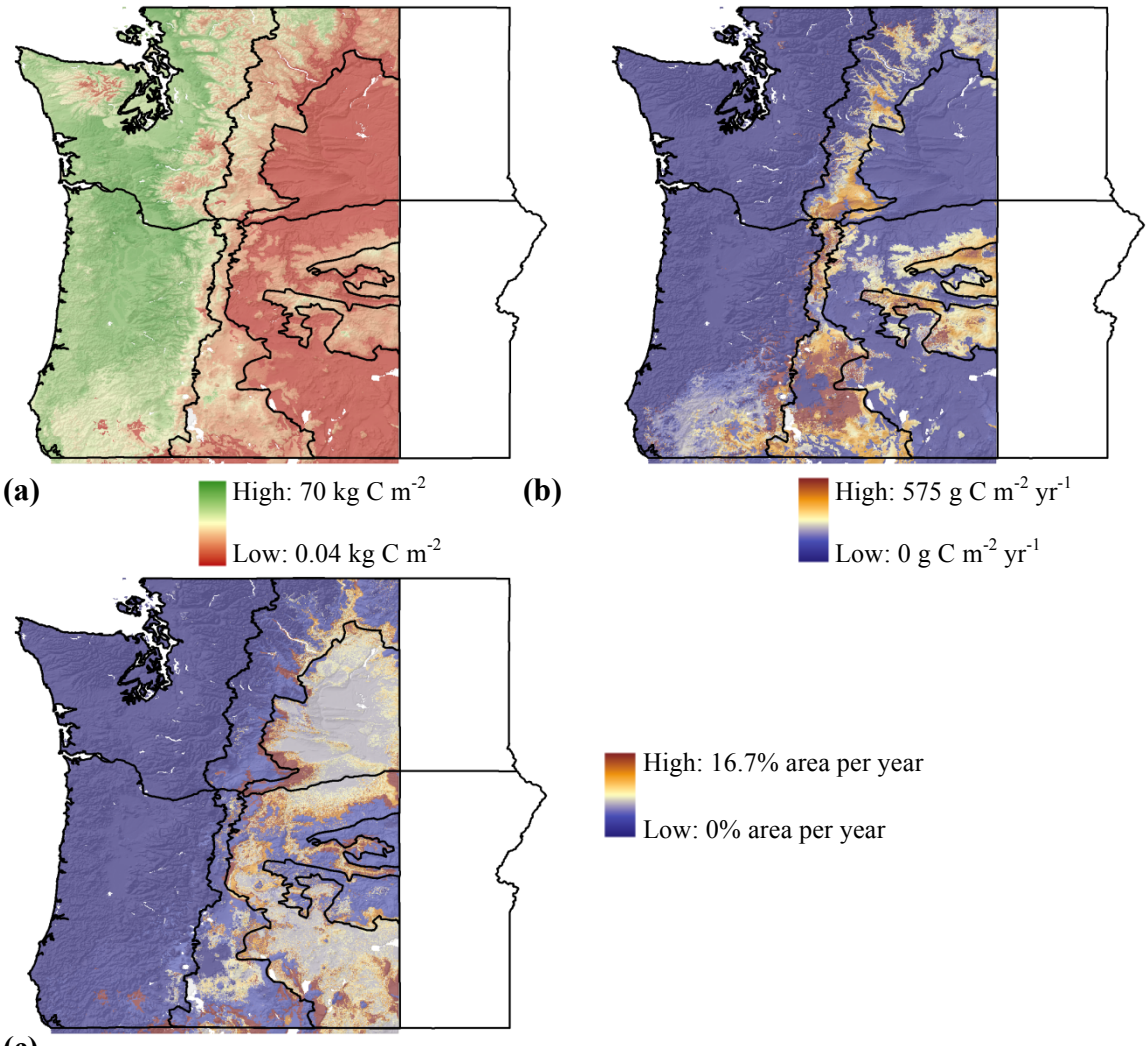

Fig 3. MC1 simulated 1971-2000 mean (a) total ecosystem carbon, (b) carbon consumed by fire, and (c) burn area

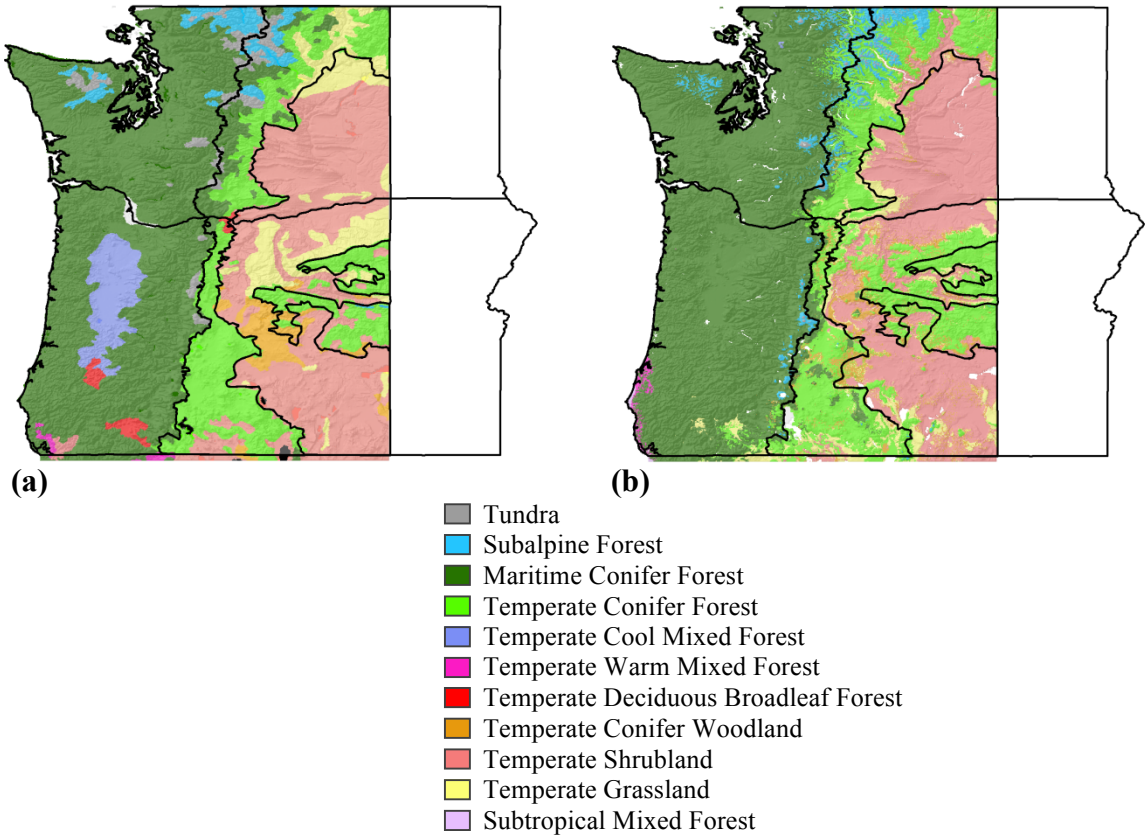

Fig 4. (a) Kuchler (1975) potential vegetation map and (b) 1971-2000 simulated modal vegetation types.

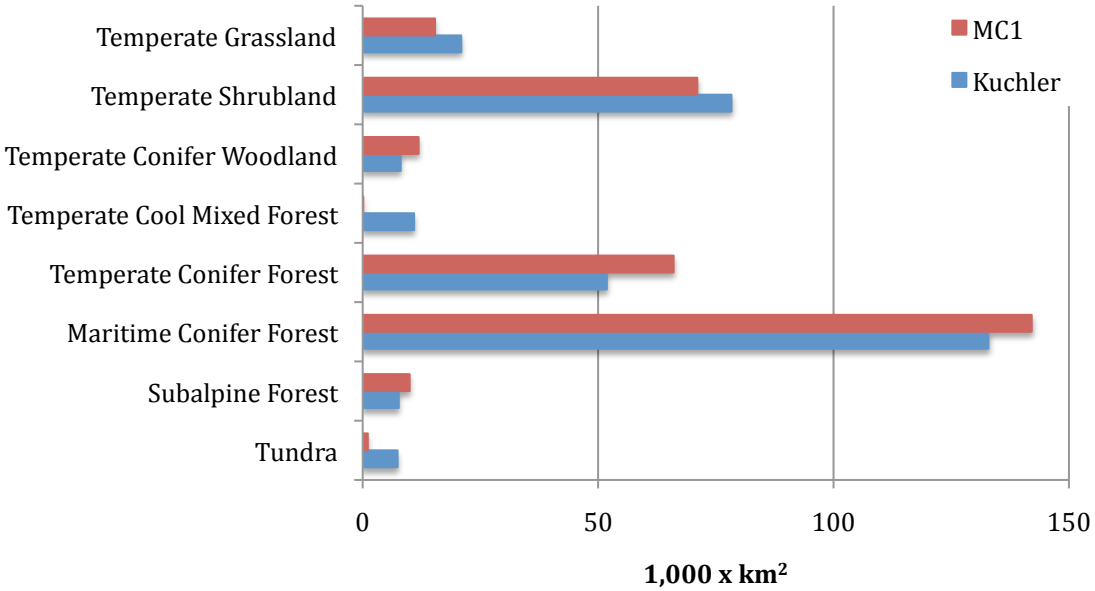

Fig 5. Comparison of historical vegetation areas between map from Kuchler (1975) and MC1-simulated vegetation distribution

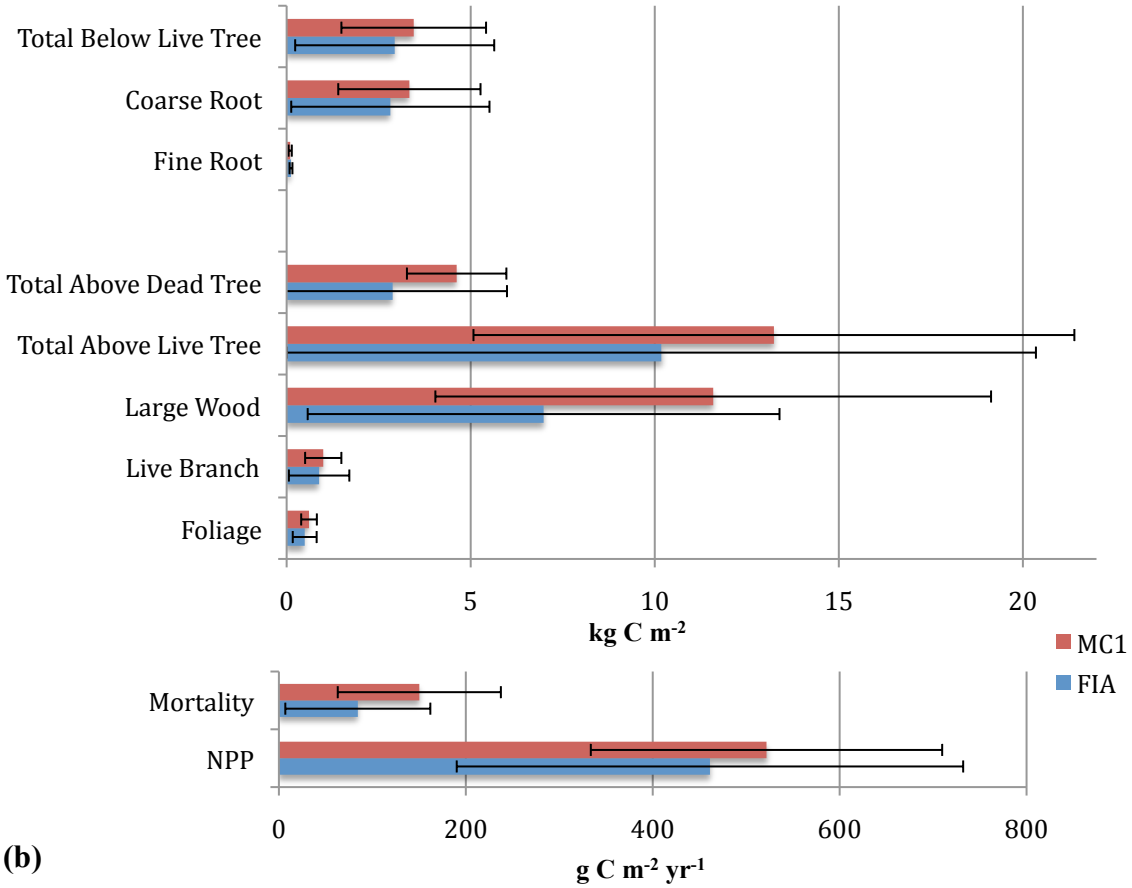

Fig 6. Comparison of carbon (a) pools and (b) fluxes between MC1 and periodic FIA plots across Oregon from Hudiburg et al. (2009). Error bars denote +/- one standard error. The FIA database contained 5,093 plots, 89.4% on public lands, with stand ages of 212 +/- 134 years (mean +/- standard error).

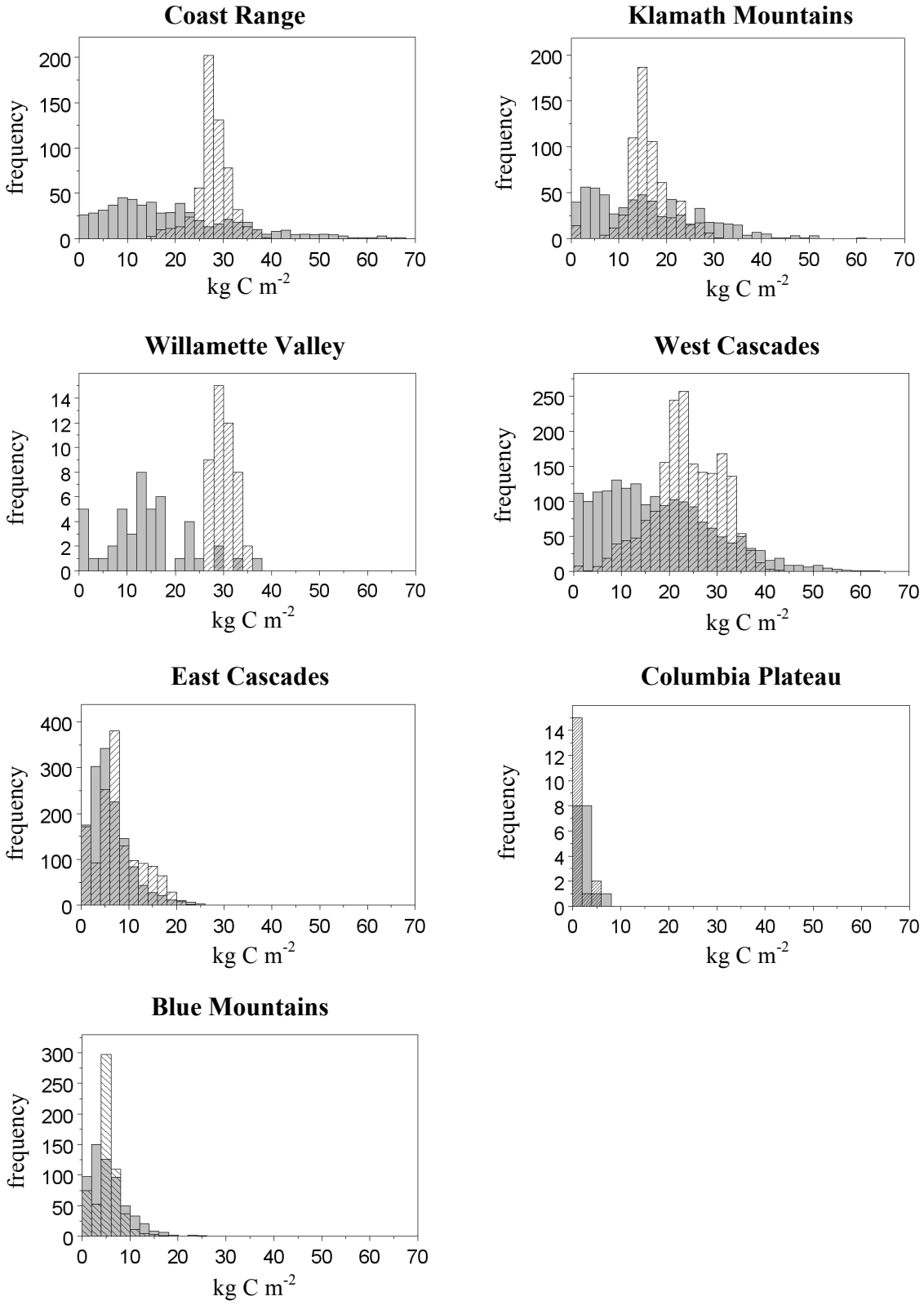

Fig 7. Histograms of total live carbon in FIA plots across Oregon from Hudiburg et al. (2009) and MC1. MC1 values were taken from the grid-cell containing each plot.

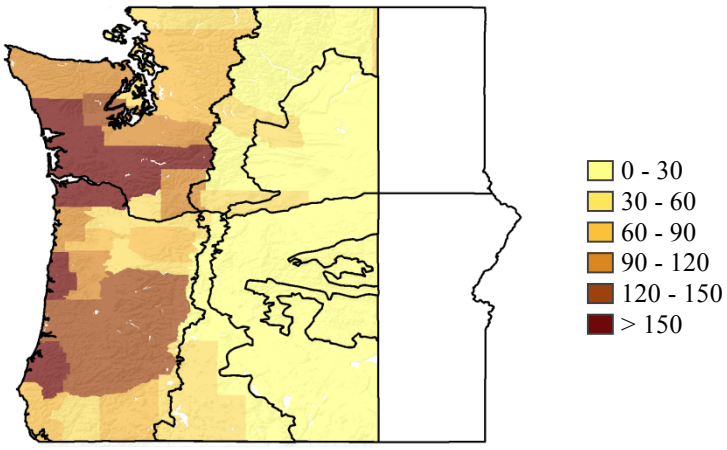

Fig 8. Average timber removals by county from 1965-2002 in g C m^{-2} yr^{-1}. Data obtained from Washington State DNR (2009) and Oregon Department of Forestry (2009).

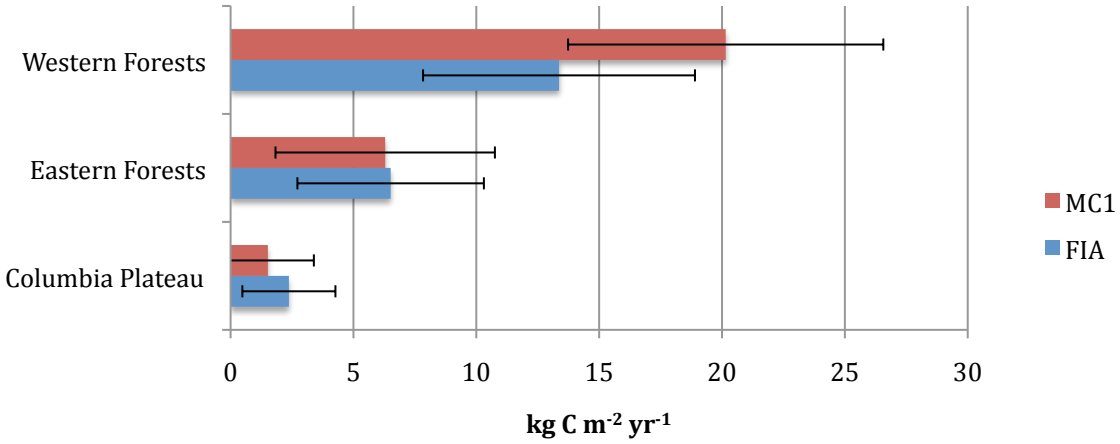

Fig 9. Comparison of historical aboveground live forest carbon between MC1 and interpolated FIA map from Blackard et al. (2008) by region. Error bars denote +/- one standard error.

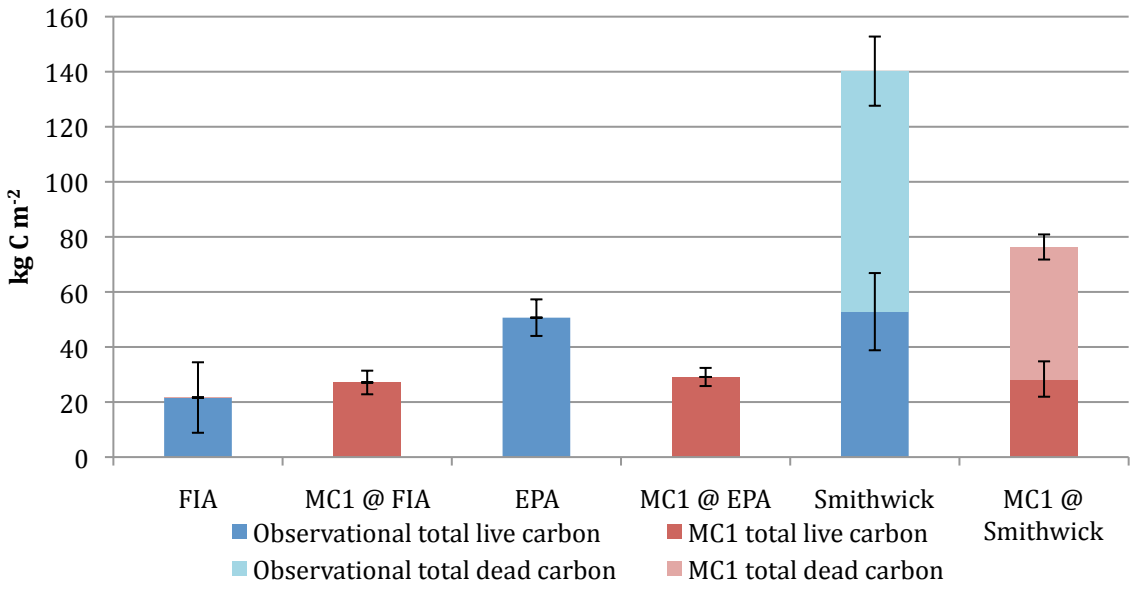

Fig 10. Comparisons of carbon pools between old-growth observational plots and MC1 run without fire in the Western Forests region. Error bars denote +/- one standard error. FIA and EPA plot data are from Hudiburg et al. (2009). Only data from Smithwick et al. (2002) contain total dead carbon. FIA data contain 1,607 plots, 98.2% on public lands, with stand ages of 332 +/- 123 years (mean +/- standard error). EPA data contain eight plots on public lands with stand ages of 417 +/- 215 years. Smithwick data contain 37 plots on public lands with stand ages of 429 +/- 257 years.

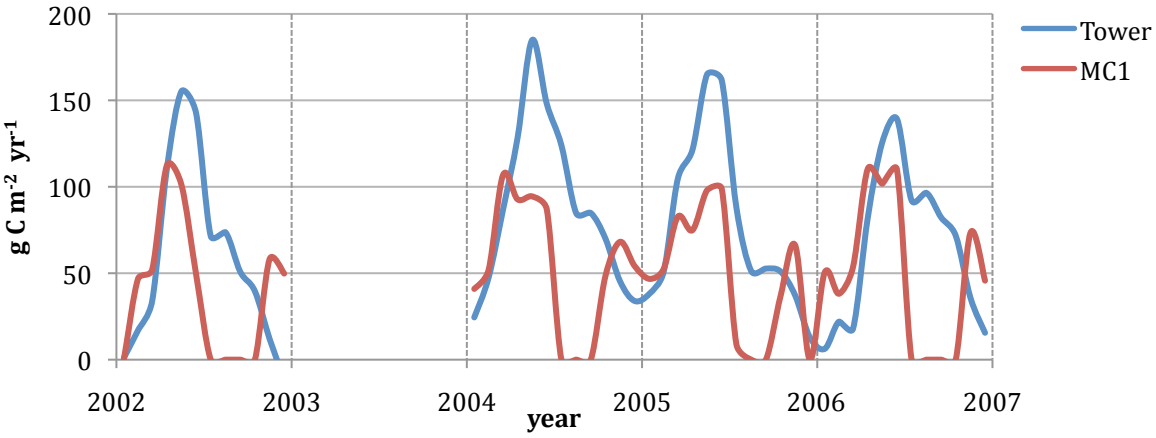

Fig 11. Comparison of NPP seasonality between MC1 and data derived from flux measurements at the Metolius "intermediate pine" site tower (44.4523° lat, -121.5574° lon, Law 2007). Observed data were missing for 2003. The site was clear-cut in 1917, and we simulated a clear-cut in MC1 during the same year.

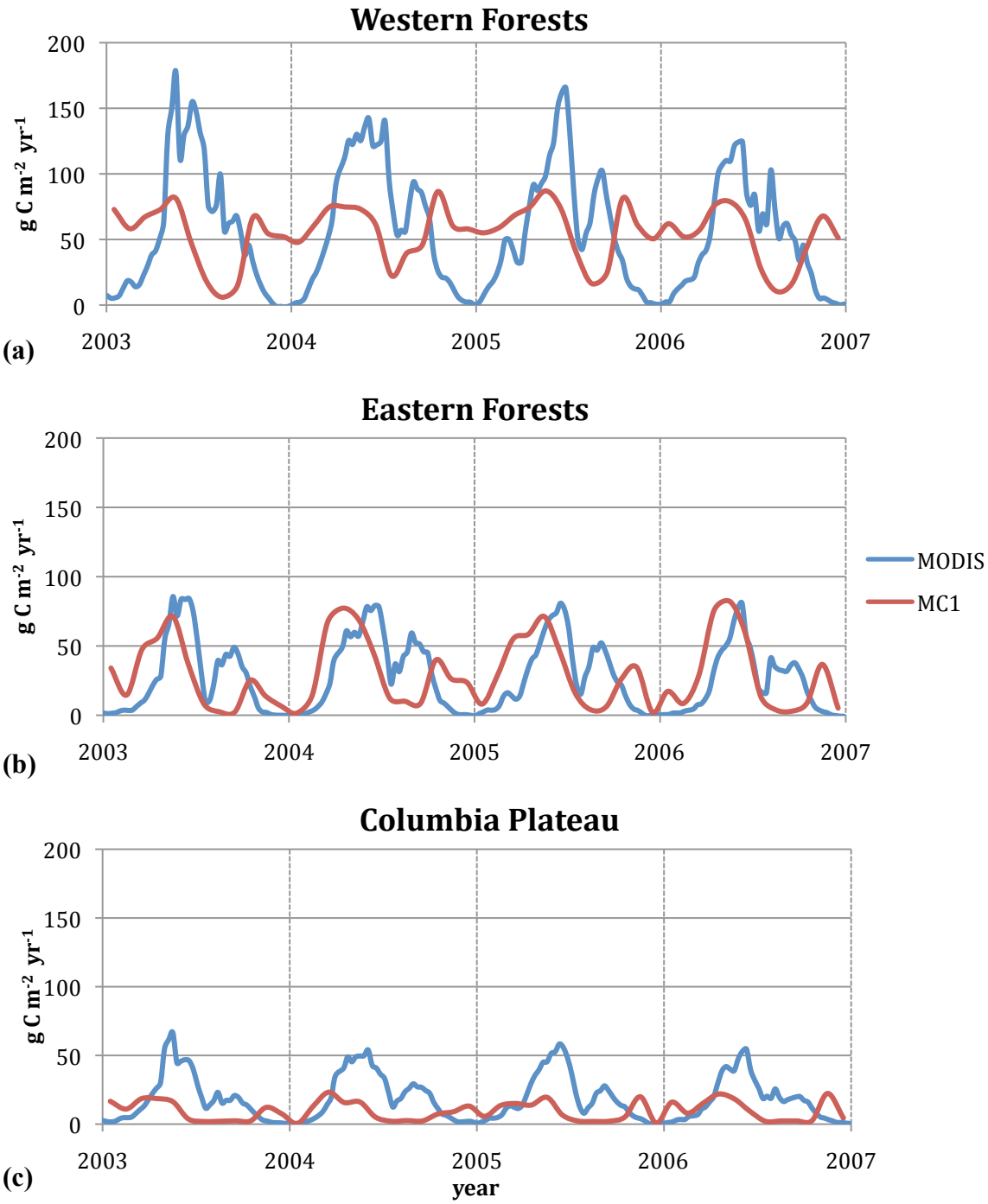

Fig 12. Comparison of NPP seasonality between MC1 and MODIS Aqua satellite data over the (a) Western Forests, (b) Eastern Forests, and (c) Columbia Plateau regions. Values were averaged over all grid cells in each corresponding domain. A 24-day filter was applied to the MODIS data.

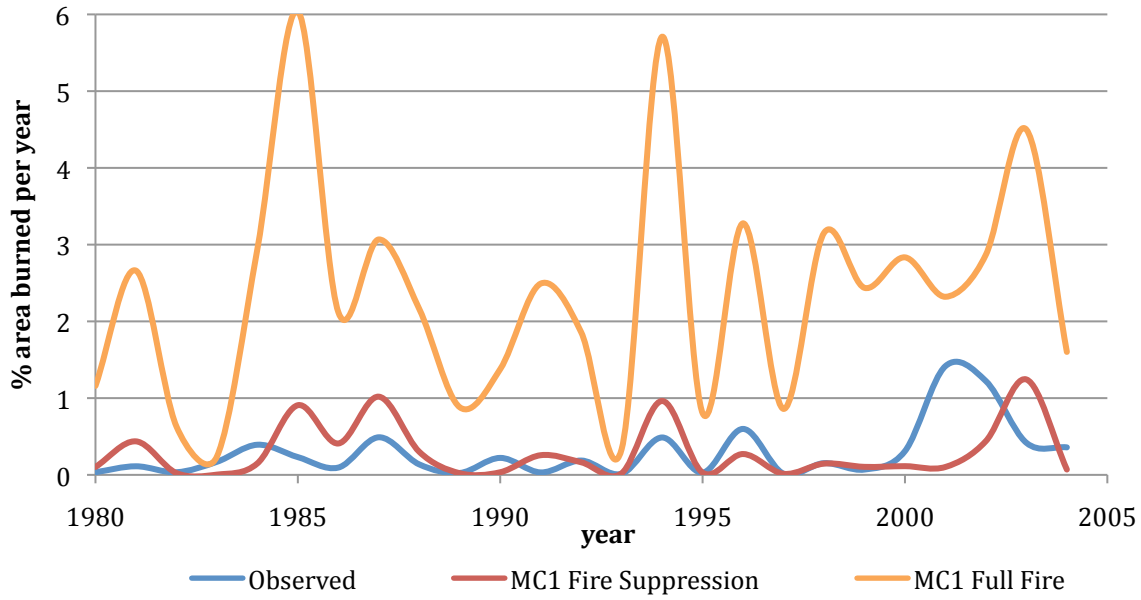

Fig 13. Comparison of annual area burned between observed data (Westerling et al. 2003) and MC1. Time series are shown for MC1 simulations with full fire and fire suppression.

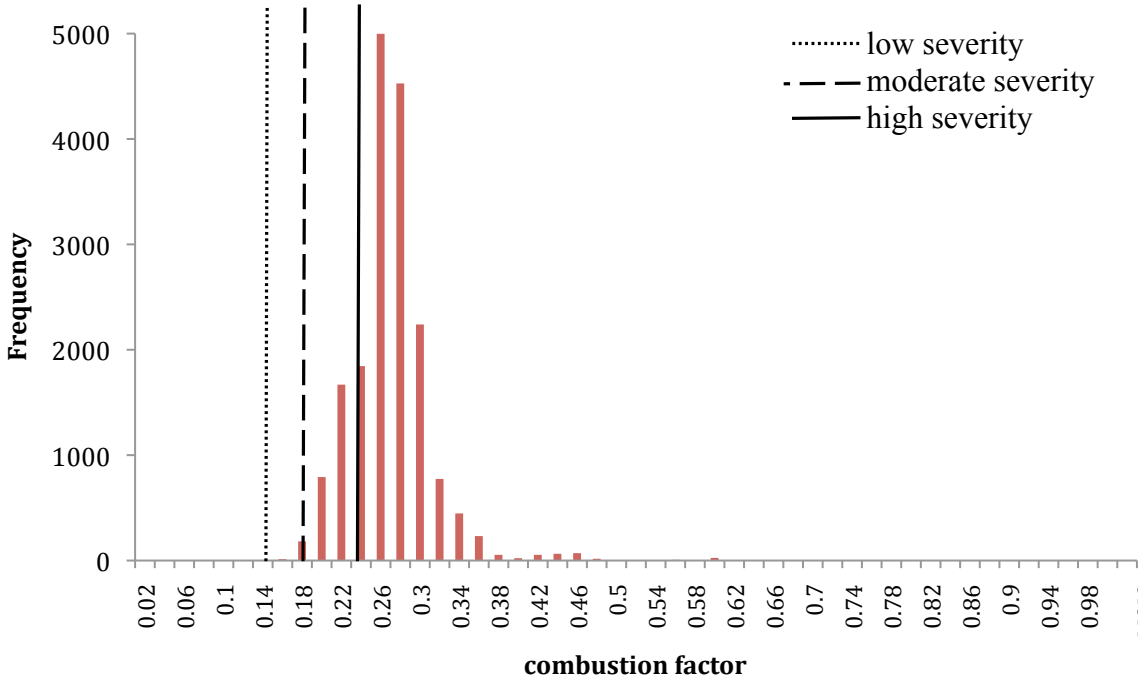

Fig 14. Histogram of MC1 combustion factors (fraction of pre-burn mass lost to combustion in fire) in the Klamath Mountains ecoregion during 2002. Overlaid vertical bars are combustion factors from 2002 Biscuit fire from Campbell et al. (2007) for low, moderate, and high severity fires. Factors were mass-weighted for trees, shrubs, snags, non-woody biomass, 1-hour fuels, 10-hour fuels, 100-hour fuels, 1000-hour fuels, litter, and duff.

Table 2: Domain-wide mean annual climatic variables for the historical and nine future climates. Values in parentheses denote absolute changes for temperature and percent changes for precipitation and vapor pressure deficit.

Scenario	**Precipitation** (cm H_2O yr^{-1})	**Temperature** (°C)	**Vapor Pressure Deficit** (Pa)
Historical	118.2	8.4	453.4
CSIRO B1	122.4 (+3.6)	9.8 (+1.4)	523.9 (+15.6)
CSIRO A1B	129.8 (+9.9)	10.1 (+1.7)	520.4 (+14.8)
CSIRO A2	135.7 (+14.9)	11.0 (+2.6)	548.5 (+21.0)
MIROC B1	126.1 (+6.7)	11.6 (3.2)	564.6 (+24.5)
MIROC A1B	126.2 (+6.9)	12.3 (+3.9)	577.6 (+27.4)
MIROC A2	126.4 (+7.0)	12.6 (+4.2)	595.3 (+31.3)
Hadley B1	113.4 (-4.0)	11.2 (+2.8)	644.8 (+42.2)
Hadley A1B	107 (-9.4)	12.5 (+4.1)	747.1 (+64.8)
Hadley A2	110.4 (-6.6)	12.6 (+4.2)	736.6 (+62.5)

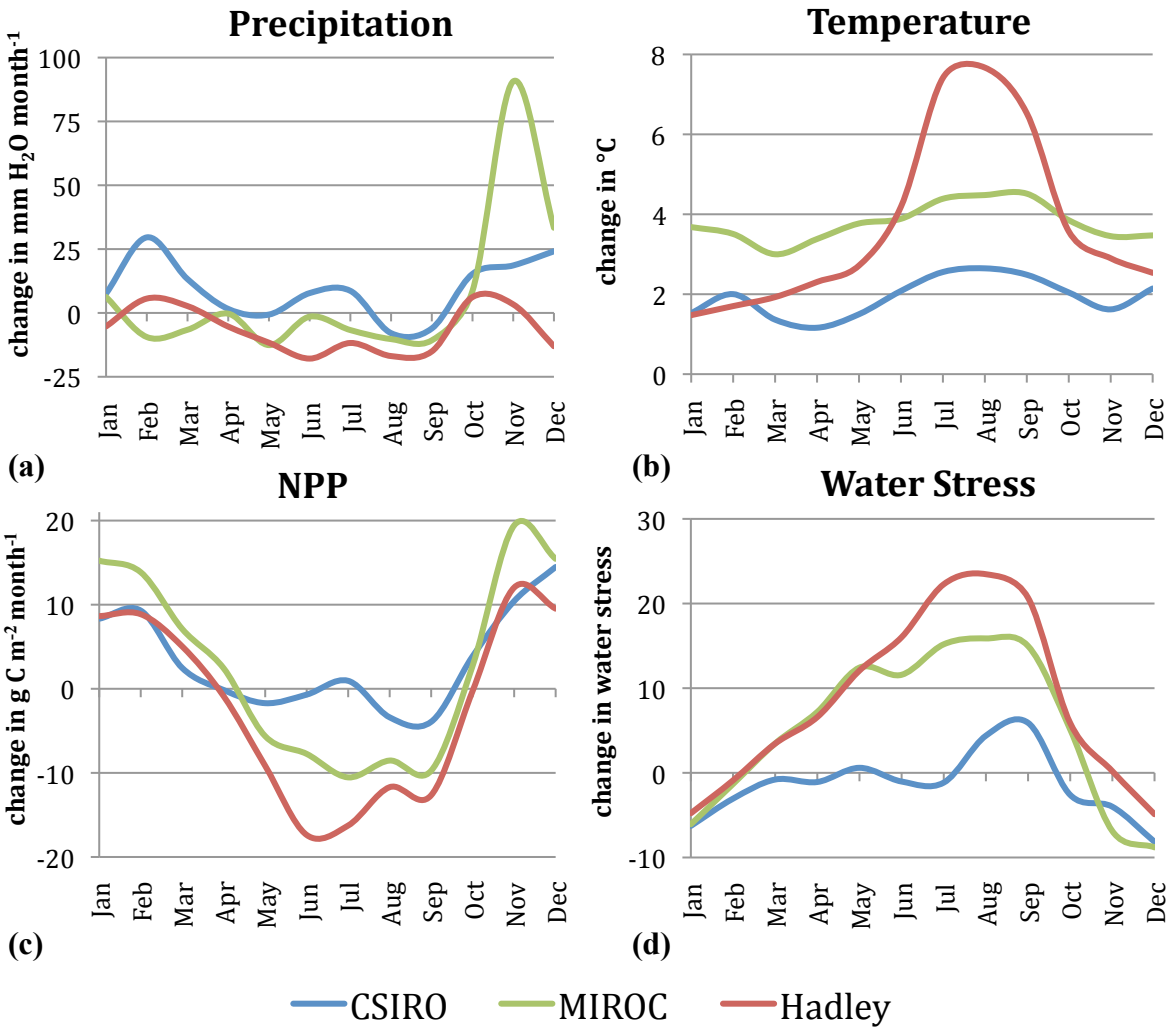

Fig 15. Future seasonal changes in projected (a) precipitation, (b) temperature, and MC1-simulated (c) NPP and (d) water stress (equation 2) for nine future climate projections, averaged by GCM.

Table 3. Measures of inter-annual and inter-decadal variability among future climate projections. σ_i = inter-annual variability, r_1 = correlation of consecutive residuals (inter-decadal variability), Z_{runs} = Z-score from runs test, p_{runs} = p-value from runs test.

Scenario	**σ_i** (inter-annual)	**r_1** (inter-decadal)	**Z_{runs}** (inter-decadal)	**p_{runs} (if $Z_{runs} < 0$)** (inter-decadal)
Historical	16.02	0.166	-2.08	0.020
CSIRO B1	19.16	-0.090	0.93	
CSIRO A1B	19.05	0.089	-0.39	0.349
CSIRO A2	19.66	-0.029	-0.42	0.339
MIROC B1	18.21	-0.160	1.28	
MIROC A1B	18.61	-0.036	0.43	
MIROC A2	16.33	0.130	-0.62	0.267
Hadley B1	15.34	0.051	-0.21	0.418
Hadley A1B	13.72	0.052	0.00	
Hadley A2	14.87	-0.024	0.14	

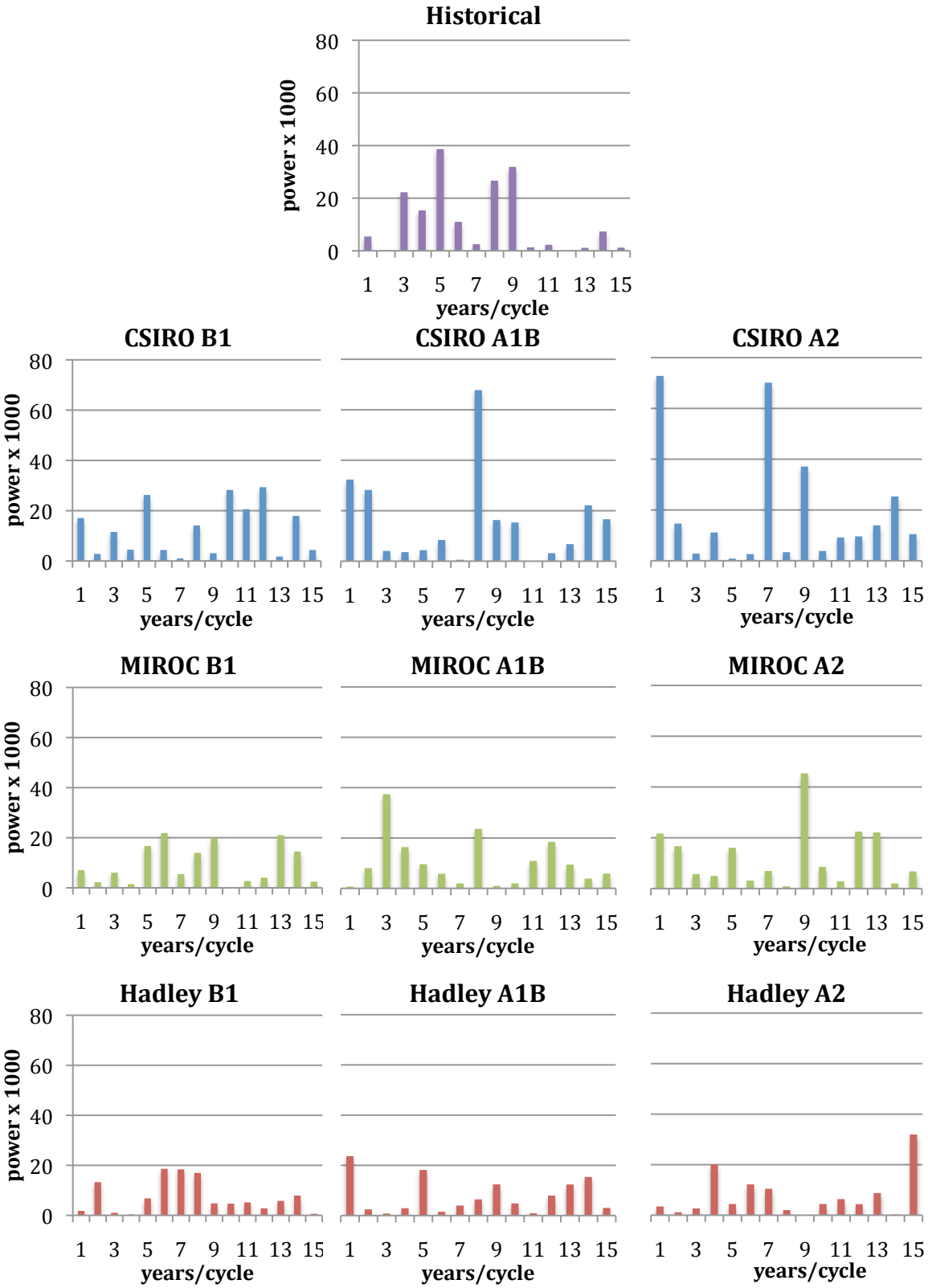

Fig 16. Powers of fast Fourier transforms on domain-averaged precipitation time-series.

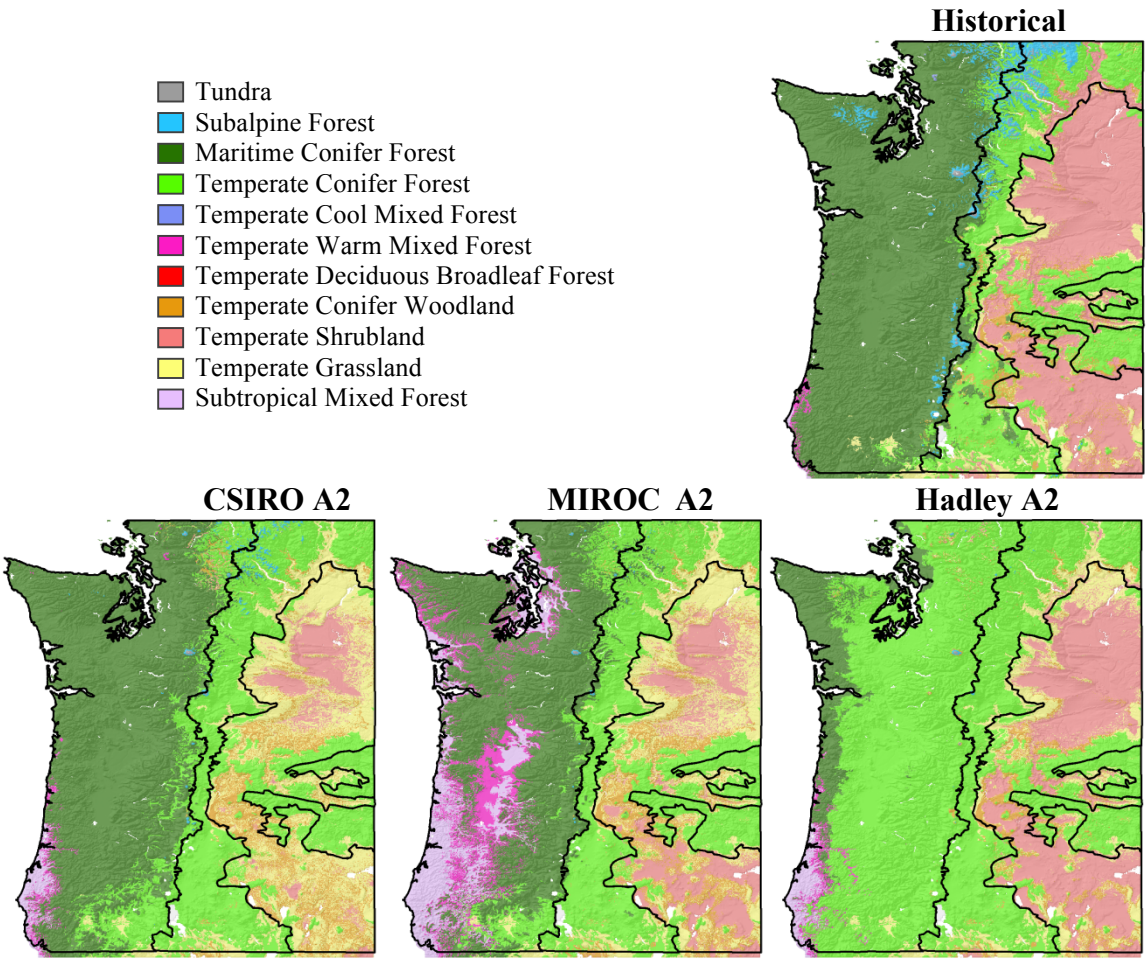

Fig 17. Mode vegetation types for historical and future A2 scenarios.

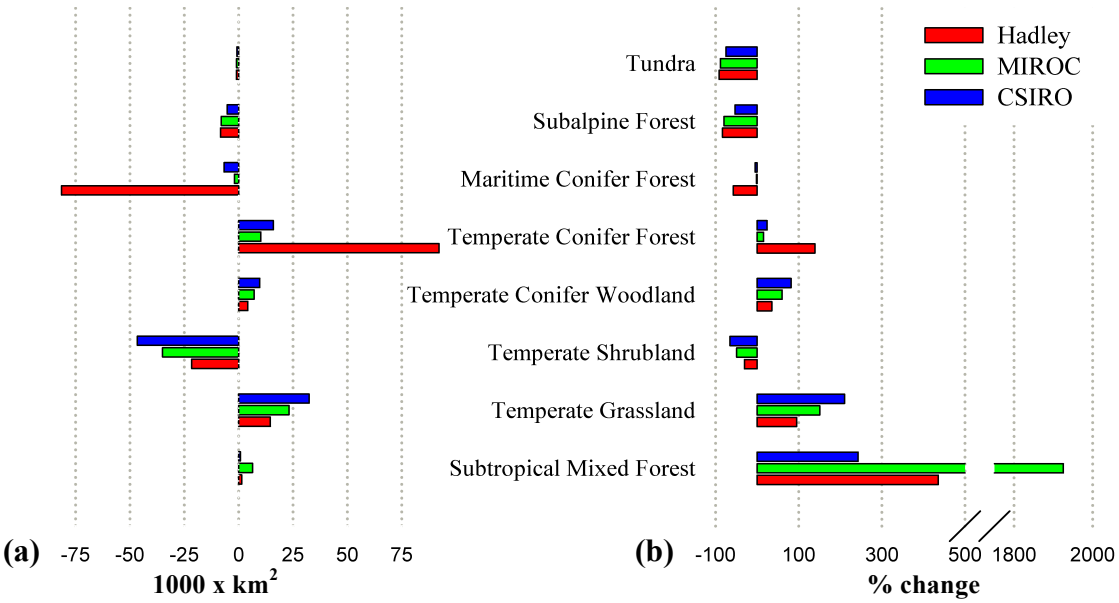

Fig 18. Changes in vegetation distributions for major vegetation types by (a) absolute area and (b) percentage cover, averaged by GCM.

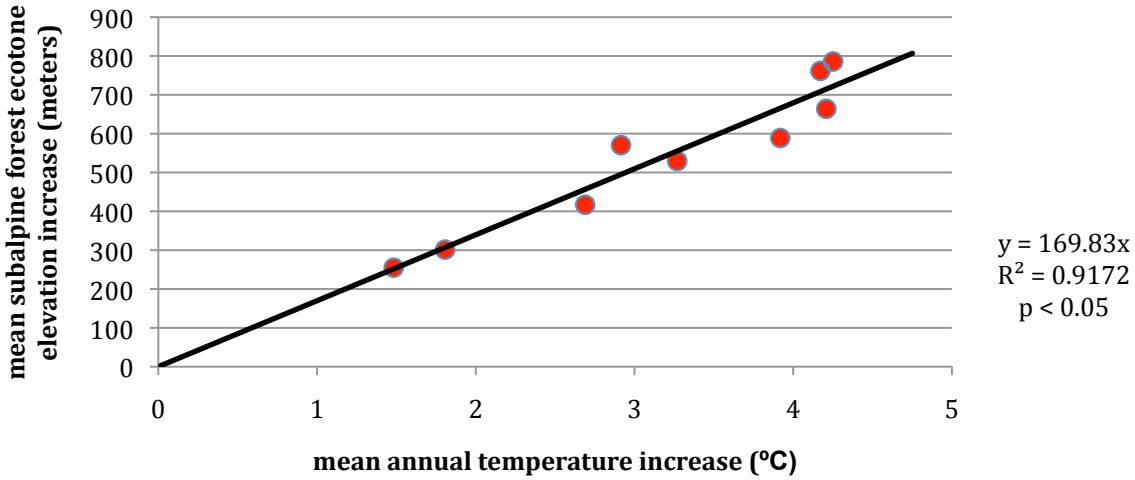

Fig 19. Mean subalpine ecotone elevation increase as a function of increases in mean annual temperatures for future scenarios.

Table 4. Historical and future carbon and fire values by region. Future scenarios are averaged by GCM. Percent changes from historical are given in parentheses.

Region	Scenario	Total Ecosystem Carbon (kg C m^{-2})	Biomass Consumed by Fire (g C m^{-2} yr^{-1})	Burn Area (% area burned per year)
All Domain	Historical	27.7	16.5	2.2
	CSIRO	27.4 (-1.2)	30.1 (+82.2)	3.8 (+74.0)
	MIROC	27.9 (+0.8)	20.2 (+22.2)	3.2 (+47.5)
	Hadley	23.7 (-14.5)	59.3 (+258.5)	3.5 (+58.6)
Western Forests	Historical	46.1	6.6	0.2
	CSIRO	45.0 (-2.4)	29.2 (+344.1)	0.7 (+206.6)
	MIROC	45.6 (-1.1)	9.2 (+39.4)	0.3 (+28.5)
	Hadley	37.9 (-17.7)	94.1 (+1,332.6)	1.9 (+713.6)
Eastern Forests	Historical	20.7	41.6	2.7
	CSIRO	21.1 (+1.9)	51.7(+24.3)	3.6 (+33.0)
	MIROC	22.3 (+7.9)	49.2 (+18.3)	3.5 (+28.6)
	Hadley	19.3 (-6.4)	52.8 (+26.9)	3.5 (+29.8)
Columbia Plateau	Historical	5.6	11.9	4.7
	CSIRO	5.9 (+4.9)	14.8 (+24.2)	8.7 (+84.9)
	MIROC	5.8 (+3.9)	14.1 (+18.9)	7.5 (+59.2)
	Hadley	5.7 (+1.4)	12.2 (+2.9)	5.8 (+23.1)

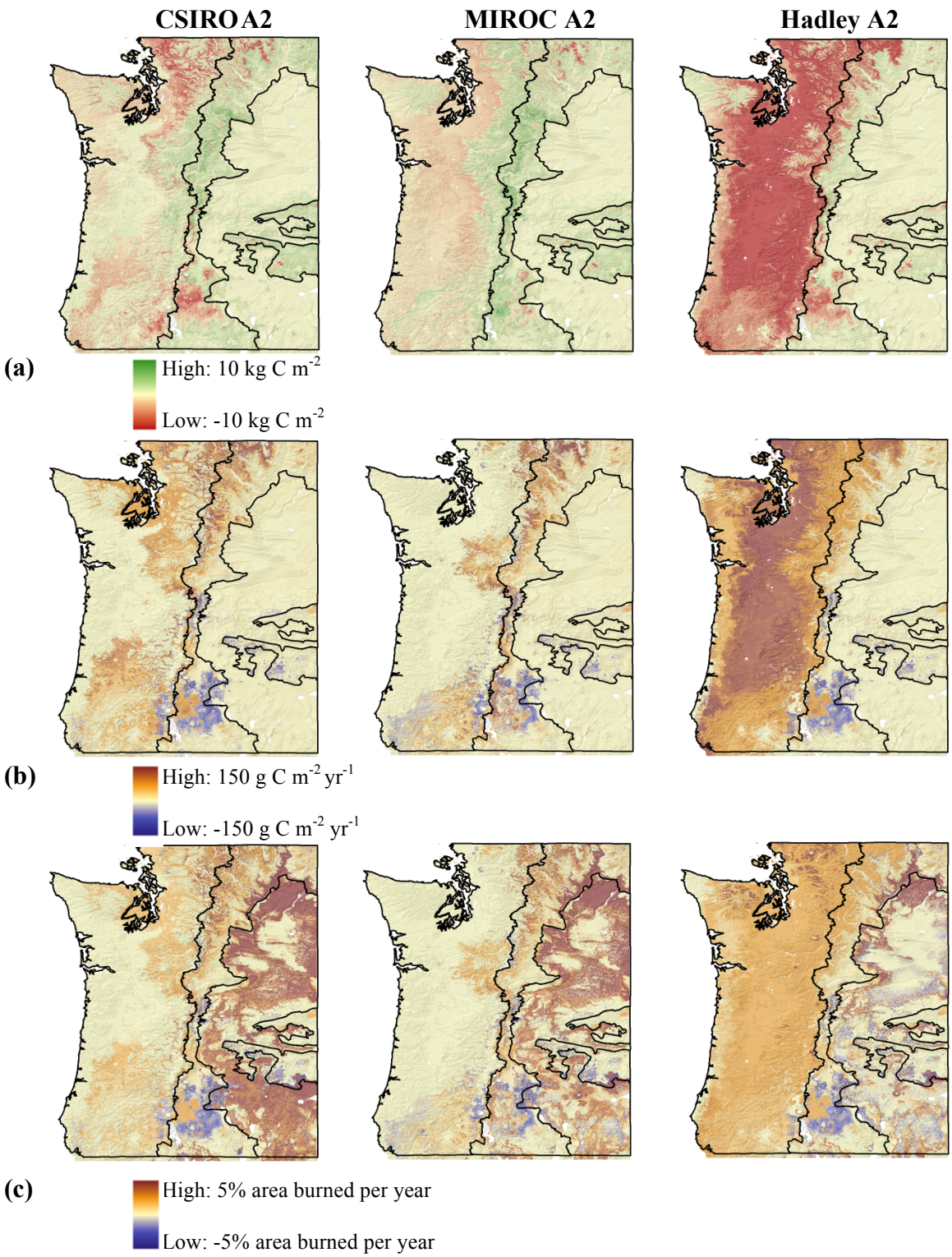

Fig 20. Changes in future means of (a) total ecosystem carbon, (b) biomass consumed by fire, and (c) area burned for A2 scenarios.

Table 5. Spatial correlation coefficients between changes in biomass combusted and total ecosystem carbon.

Scenario	Correlation Coefficient
CSIRO B1	-0.33091
CSIRO A1B	-0.25075
CSIRO A2	-0.39889
MIROC B1	-0.16288
MIROC A1B	-0.06674
MIROC A2	-0.02164
Hadley B1	-0.76812
Hadley A1B	-0.78942
Hadley A2	-0.79113

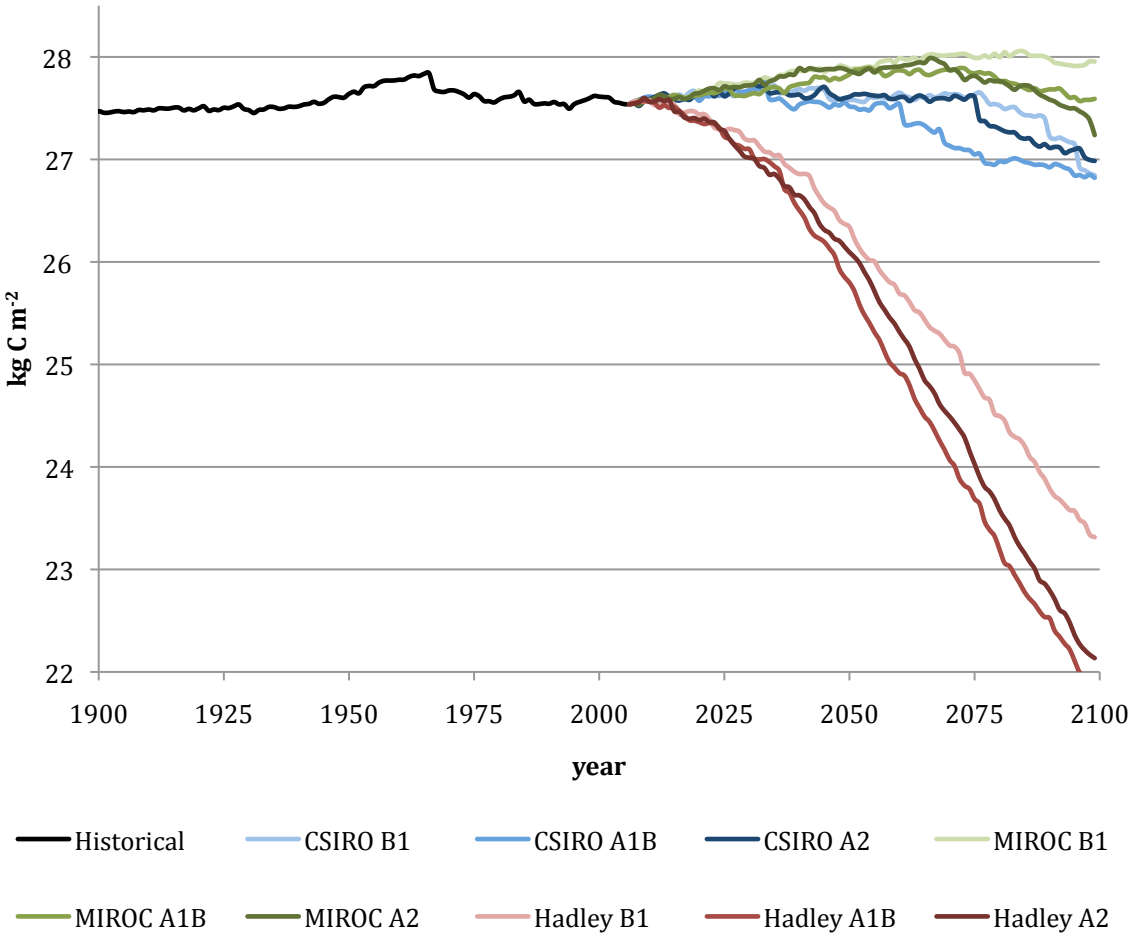

Fig 21. Time series of domain-averaged total ecosystem carbon for historical and future simulations.

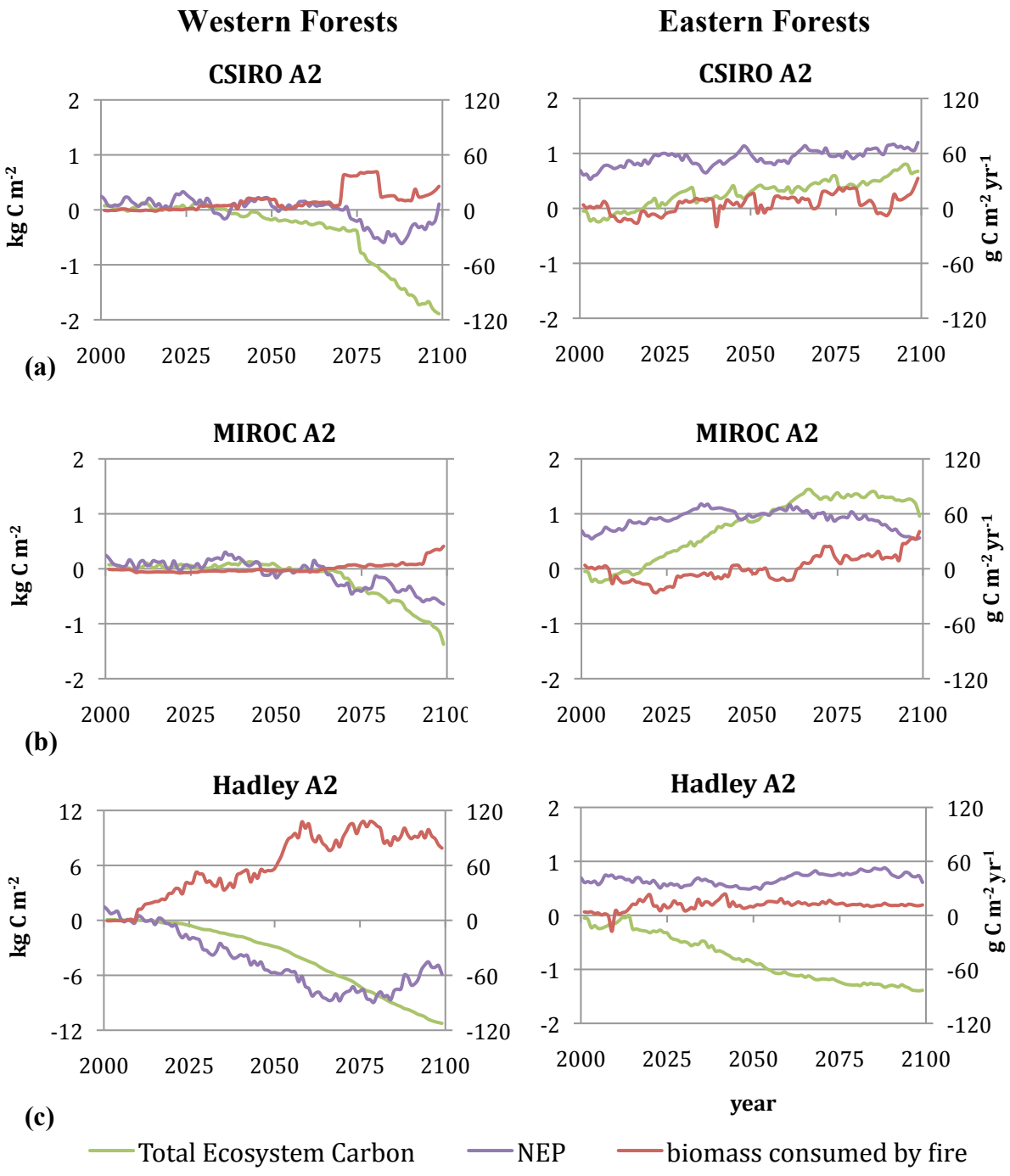

Fig 22. Time series of total ecosystem carbon, net ecosystem production (NEP), and biomass consumed by fire for (a) CSIRO A2, (b) MIROC A2, and (c) Hadley A2, averaged across the Western and Eastern Forests regions. Ecosystem carbon and biomass consumed by fire are plotted as differences from 1971-2000 means. 11-year filters were applied to biomass consumed by fire and NEP, which are plotted on the right-hand axis. Note the change of scale for Hadley A2 western forests.

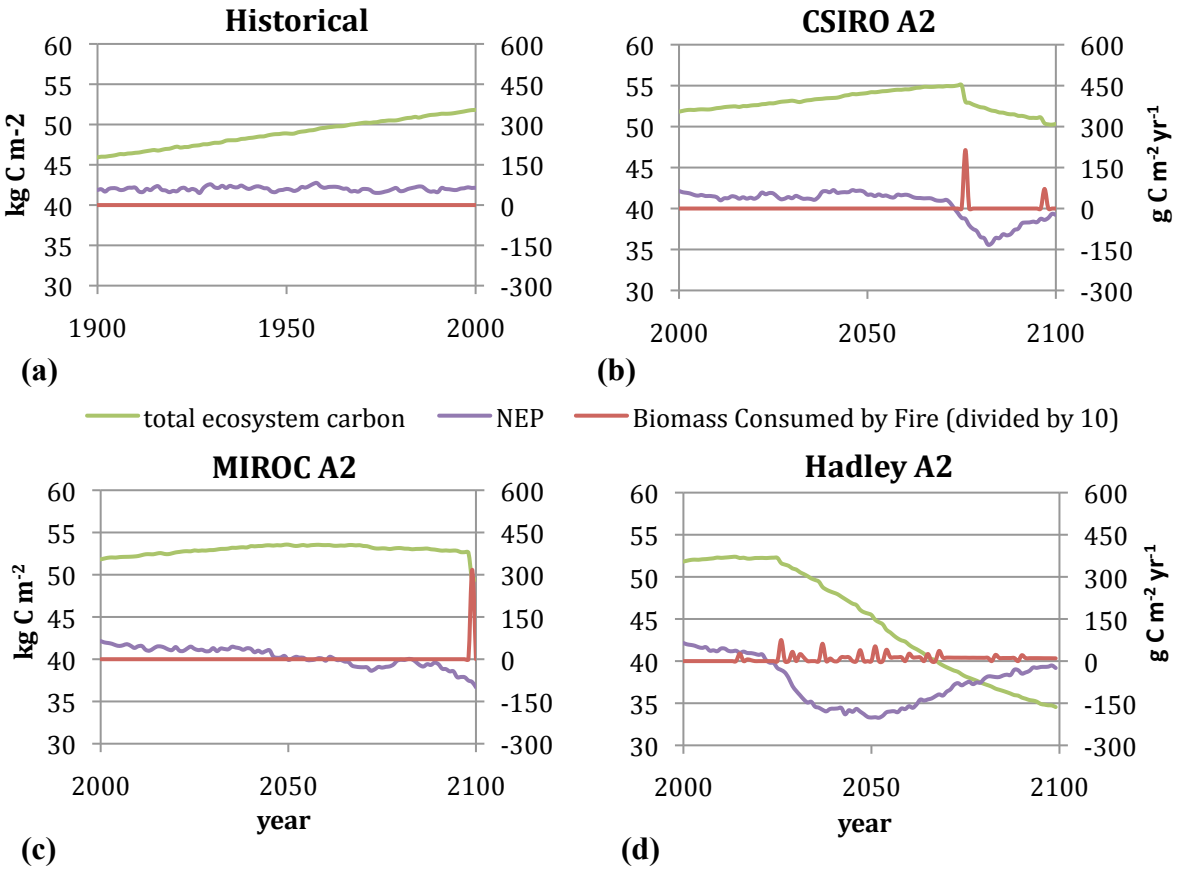

Fig 23. Time series of ecosystem carbon, NEP, and biomass consumed by fire for (a) Historical, (b) CSIRO A2 , (c) MIROC A2, and (d) Hadley A2 on single grid-cell in West Cascades ecoregion (47.2417° latitude and -121.591° longitude). NEP and biomass consumed by fire are plotted on the right-hand axis. An 11-year filter was applied to NEP values, and biomass consumed by fire values were divided by 10 to display on the same axis.

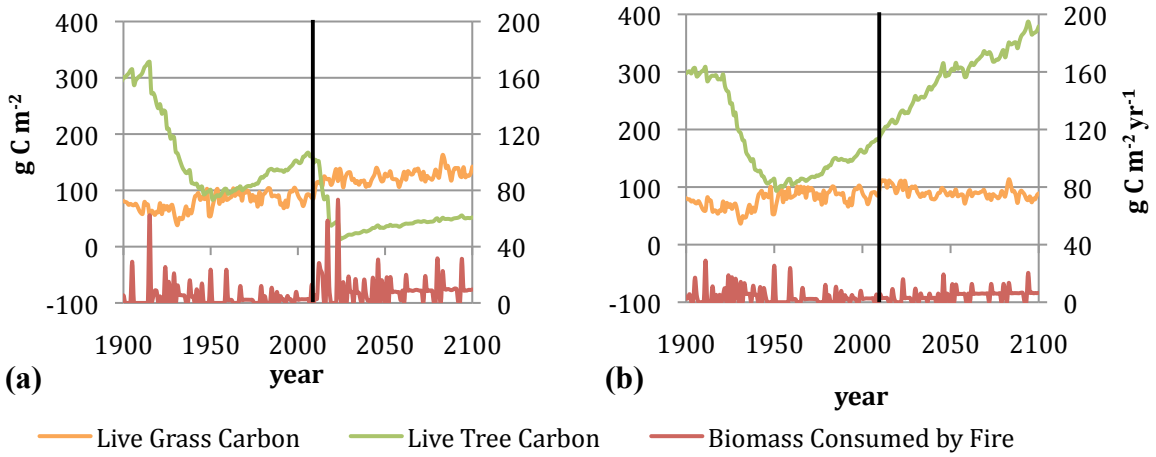

Fig 24. Time series of grass and tree carbon, and biomass consumed by fire, for two adjacent grid-cells simulated under CSIRO A2. (a) 43.34° latitude, -120.375° longitude, (b) 43.425° latitude, -120.383° longitude. The vertical lines indicate the start of future simulation. Biomass consumed by fire is plotted on the right-hand axis.

Table 6. Domain-averaged carbon and fire variables under sensitivity analyses. Percent changes from the historical period are given in parentheses. Future fire suppression and no-fire runs were compared against historical runs with the same fire prescription.

Sensitivity Analysis	Scenario	Total Ecosystem Carbon (kg C m^{-2})	Biomass Consumed by Fire (g C m^{-2} yr^{-1})	Burn Area (% area burned per year)
Control	Historical	27.7	16.6	2.2
	CSIRO A2	27.4 (-1.0)	31.6 (+90.7)	3.9 (+79.0)
	MIROC A2	27.8 (+0.4)	25.3 (+52.4)	3.4 (+54.0)
	Hadley A2	23.5 (-15.2)	62.5 (+277.5)	3.5 (+57.1)
Suppressed Fire	Historical	28.1	9.4	0.28
	CSIRO A2	29.0 (+3.1)	26.6 (+182.0)	0.68 (+144.9)
	MIROC A2	29.3 (+4.2)	21.4 (+127.3)	0.58 (+110.4)
	Hadley A2	24.6 (-12.5)	60.8 (+544.2)	1.38 (+373.5)
No Fire	Historical	35.0	0.0	0.0
	CSIRO A2	35.8 (+2.4)	NA	NA
	MIROC A2	35.2 (+0.7)	NA	NA
	Hadley A2	35.5 (+1.3)	NA	NA
β-factor = 0.0	CSIRO A2	27.3 (-1.4)	31.6 (+91.2)	3.8 (+72.3)
	MIROC A2	27.7 (-0.1)	25.3 (+52.9)	3.2 (+45.0)
	Hadley A2	23.4 (-15.6)	62.7 (+279.2)	3.3 (+49.2)
β-factor = 0.6	CSIRO A2	27.6 (-0.2)	30.9 (+86.4)	4.2 (+89.9)
	MIROC A2	28.1 (+1.4)	24.6 (+48.6)	3.7 (+68.6)
	Hadley A2	23.6 (-14.6)	61.3 (+270.2)	3.8 (+74.8)
three year precipitation filter	CSIRO A2	28.2 (+1.7)	26.4 (+59.4)	3.8 (+70.7)
five year precipitation filter	CSIRO A2	28.4 (+2.4)	24.3 (+46.5)	3.6 (+65.1)

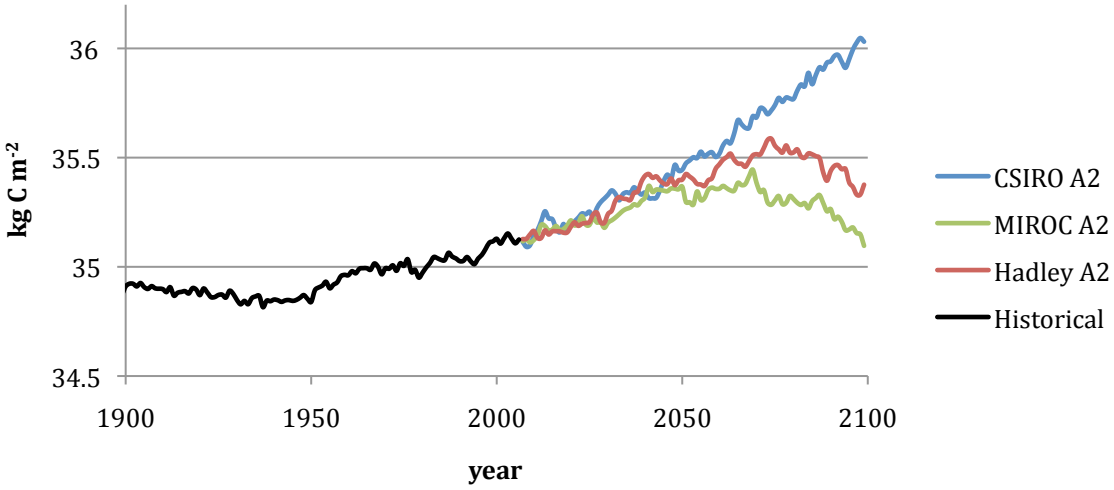

Fig 25. Time series of domain-averaged total ecosystem carbon for MC1 fire-off sensitivity analysis simulations under historical and future A2 climates.

Discussion

MC1 captured the historical spatial patterns of vegetation well. Differences between MC1 and Kuchler (1975) occurred mainly in areas of heavy human influence (Willamette Valley) and sensitivity to land cover conversion (Columbia Plateau). MC1 overestimated burn area by a factor of about eight when compared with Westerling et al. (2003). However, with the new fire suppression rule activated, it accurately simulated burn area and showed skill in capturing temporal patterns. MC1 generally overestimated carbon stocks in the Western Forests region, which has been subject to substantial human influence via logging and land conversion, and underestimated carbon stocks in the Eastern Forests and Columbia Plateau, where fire suppression has caused an increase in ecosystem carbon. MC1 displayed a bias in the seasonality of NPP towards decreased summer and increased winter production. This suggests the model's productivity equations may be overly sensitive to low soil moisture and under-sensitive to low temperatures, which could carry implications for future predictions.

Future climate projections used in this study displayed marked differences in the seasonality and magnitudes of changes, but also some overarching similarities. Temperatures rose ubiquitously with larger increases in summer than winter. Maximum temperatures increased more than mean temperatures, which increased more than minimum temperatures. Because of difficulties in parameterizing sub-grid cloud physics and dynamics (Washington and Parkinson 2005), future climates disagreed on the sign of precipitation changes. However, they agreed that increases occur in the winter and decreases occur in the summer. These projections, along with the conclusion that GCMs contribute greater variability than do emission scenarios, qualitatively agree with the suite of downscaled climates for the PNW in Mote et al (2008). Together, these changes lengthened the growing season, amplified the already strong seasonal cycles of precipitation and temperature, increased summer drought, and intensified the year-to-year variability of precipitation in the PNW.

Across the domain, we saw an amplification of the seasonal cycle of NPP and water stress. However, simulated ecosystem responses in the three aggregated regions varied widely depending on their mean climate, historical vegetation, and structural

inertia. The high-biomass Western Forests were largely unable to benefit from increased winter precipitation because, as has been observed (Harr 1977, Jones and Grant 1996, Mote et al. 2003), the soils were saturated in winter months. Production increased in the fall, winter, and spring because temperatures increased when soils were wet. However, the region was vulnerable to large wildfires and carbon loss under CSIRO and Hadley climates. In all cases, large fires were simulated in years with summer droughts substantially worse than what the region experienced historically (measured by soil moisture, vapor pressure deficit, and associated water stress). Here it was not fuel production, but fuel moisture that limited fires. These droughts occurred nearly every year in Hadley projections, and occurred more erratically in CSIRO projections because of its high inter-annual variability of rainfall. The affect of summer drought was also exacerbated by higher winter and spring production, which generally left the soil column more water-depleted by early summer.

The Western Forests also experienced some large-scale forest conversions: from maritime coniferous to subtropical coniferous and warm mixed forests under MIROC projections, and to temperate coniferous forests under Hadley climates. Subalpine forests were loss across all scenarios. These forest types are based on climatic indices in MC1. Mean winter temperatures are used to distinguish between temperate and subtropical forests, which are limited by frost frequency. A continentality index indicates the range of seasonal temperatures and is used to distinguish between temperate and maritime forests, which are assumed to predominate where seasonal temperatures are damped. Subalpine forests predominate in places with a relatively short growing season. Although conversions between these forest types are associated with time lags in MC1, real-world conversions display highly varying time lags associated with species-specific seedling dispersion and establishment, competition, and disturbances not simulated in MC1, such as windthrow, pests, and pathogens. We must therefore interpret these forest conversions in the context of local factors, such as the availability of new species' seed sources, likely migration pathways, successional status, and both real-world disturbance history and simulated potential for future disturbances. In general, disturbance will facilitate vegetation conversion (Overpeck et al. 1990, Neilson 1993, Whitlock et al. 2003).

Taken together, MC1 simulates major biome changes in the Western Forests that are similar to what the region experienced sometime between 12,000 and 3,5000 years ago (Whitlock 1992, Whitlock et al. 2003). During that period, summer drought was exacerbated and the region saw an expansion of early to mid-successional xerophytic taxa and higher-frequency fires that were important in maintaining the vegetation communities. In MC1, these simulated biome changes began at different times in the 21st century under the different climate projections. Hadley projections resulted in major changes as soon as 2015, whereas no major changes were seen under CSIRO and MIROC climates until about 2070. In all cases, however, the transition between biomes in the Western Forests was a lengthy process because of the high replacement inertia of these forests. We must also be aware that MC1's seasonal bias in NPP may be most important in this region because of the large effect of increases in summer drought.

Unlike the Western Forests, the Eastern Forests appeared relatively resilient to climate change. The region benefitted more from increases in winter precipitation than did the Western Forests because the rain recharged soil water in time for the growing season. The Eastern Forests were also more limited by cold temperatures during the greater winter months, and experienced greater temperature increases under our future climates than did the Western Forests. Eastern Forest winter NPP values were therefore significantly elevated. Although summer NPP was decreased and fire activity increased, the region remained relatively carbon-neutral across scenarios and any carbon changes approached equilibrium by 2100. This reflects the legacy that frequent historical fires left on ecosystem structure and function. However, our fire suppression sensitivity analysis suggests historical fire suppression has predisposed the region to greater increases in future fires.

The Columbia Plateau is severely limited by water. Under all scenarios except Hadley A1B and A2, which show minor losses, precipitation increased in the region. This, along with an increasing synchrony between high temperatures and wet soil in the greater winter months, led to substantial increases in tree and grass productivity. Because of its overall low productivity and dry summers, fires in the Columbia Plateau were mainly limited by fuel contents. This is underscored by the region's insensitivity to precipitation variability and its increased fires under increasing CO_2 enrichment

sensitivity. In places where the increased fuel production sparked large fires, shrublands were converted to grasslands that were then maintained by an elevated fire regime. In many places these large fires didn't occur and shrublands were converted to woodlands as woody carbon out-competed grasses for light and soil water. The region appears to currently reside on a tipping point, capable of being perturbed by both increased rainfall and winter temperatures. Woody dominance or fire feedbacks may then maintain the resulting woodlands or grasslands. Like the Eastern Forests, the Columbia Plateau may see greater increases in fire because of historic fire suppression.

Across the domain, MC1 simulated increased fire activity due to higher winter productivities and summer droughts. Domain-wide annual burn area increased by 74%, 48%, and 58%, and biomass combusted increased by 82%, 22%, and 259% under mean CSIRO, MIROC, and Hadley climates, respectively. Our reported increases in area burned are less than those in Littell et al. (2009), who reported a doubling or tripling of area burned in Washington by the 2080s, compared with the 1916-2006 mean. However, the study domains in the two studies do not completely overlap, and Littell et al. (2009) used statistical models to predict future fires.

Fire became the dominant driver of carbon losses, especially under CSIRO and Hadley climates. However, even in the absence of fire, the domain became a carbon source by 2070 under two of the three A2 projections (MIROC and Hadley). Our changes in ecosystem carbon were similar to, but lower than, those from Bachelet et al. (2004). They ran MC1 under two future climates at 0.5° resolution and reported one gain of 0.40 Pg C and one loss of 0.23 Pg C for the PNW. We report a mean carbon gain of 0.07 Pg C under MIROC climates, and losses of 0.10 and 1.26 Pg C under CSIRO and Hadley.

MC1 simulated numerous forest conversions in the Western Forests and shrubland conversions in the Columbia Plateau. Our simulated vegetation shifts are qualitatively similar to earlier MC1 output of the continental U.S. at a 0.5° resolution (Bachelet et al. 2001). Bachelet et al. (2001) reported decreases in subalpine forests and tundra, conversion of shrublands to savannas, increasing areas of mixed forests in the Western Forests, and expansion of dry temperate coniferous forests in the Eastern Forests region.

All the above results come with caveats involving model limitations and uncertainties. Major uncertainties remain in predicting anthropogenic CO_2 emissions and climatic responses, as evidenced by the divergent behavior of projected future climates. Our climate projections were constructed using a relatively simple method, the perturbation method, and cannot account for spatial subtleties such as increased warming in regions that lose snowpack (Salathe et al. 2007). Additionally, MC1 runs on a monthly time-step and may miss changes in daily climate variation, such as differential warming between day and night or temperature extremes. MC1 simulates potential vegetation and ecosystem function, separate from non-climatic human influences. Urbanization, fire suppression, harvesting, species introductions, and other human activities greatly affect ecosystem structure and function. We also found a strong seasonal NPP bias in MC1 that suggests its production is over-sensitive to summer drought and under-sensitive to low winter temperatures. Many vegetation types in MC1 rely strictly on climatic indices, such as the distinction between different types of coniferous forests. Other vegetation changes driven by fire and biomass stocks incorporate biogeochemical phenomena and progress at more predictable rates. Still, the simulated vegetation changes due to climatic thresholds are indicative of climatic conditions that promote the presence of a given physiognomic vegetation type, and may portend species migrations and the potential for ecosystems to undergo changes in composition and structure. Increases in fire and pest outbreaks may also hasten these vegetation changes.

All the above results and conclusions must be taken as preliminary. The large bias MC1 displayed in the seasonality of NPP is troubling because of the implications it may carry for our general conclusions. Because of this, we are re-calibrating the model to display a more faithful representation of monthly NPP patterns. Future analyses will include these new simulations, and some of our conclusions may change.

Conclusions

Our findings agree with paleo-data and other modeling studies that show the potential for PNW vegetation distributions and fire regimes to be strongly influenced by climate. The seasonality of precipitation in the PNW renders ecosystems vulnerable to exacerbated summer drought stress. Our results suggest the PNW may become a carbon source by the end of the 21st century due to increased drought stress, which both negatively affects productivity and increases fire activity in the western maritime forests we traditionally view as non-fire-prone. Drier forest types east of the Cascade crest appear resilient to climate change, and the arid shrublands of the Columbia Plateau and Northern Basin appear vulnerable to grassland and woodland conversion with increased rainfall and winter temperatures. Additionally, the region's forests appear more vulnerable to increases in fire than they otherwise would be because of 20th century fire suppression. However, all these conclusions are reached within the context of multiple sources of uncertainty and model biases that most likely had a strong influence on model predictions. Most prominently, MC1 did not simulate the seasonality of NPP well and this most likely carries implications for how the model reacted to increased future summer drought. We will address this issue in future publications, and our conclusions must therefore be taken as preliminary.

Although our model uncertainties are large, land managers should consider climatically-induced ecosystem changes when developing management plans. Adaptation options are still relatively limited. However, some general principles are emerging that address multiple threats. Fostering higher levels of species diversity may increase resilience to vegetation dieback, increase carbon storage, prevent against carbon storage reversals (Galik and Jackson 2009), and prevent major losses in ecosystem services during biome changes. Maintaining and establishing migration corridors may also aid in inevitable species migrations (Von Hagen 2009). As we move towards a larger and mandatory carbon credits market, managers need to consider the natural trajectory of ecosystem carbon under climate change. Our study suggests some areas may be particularly vulnerable to carbon loss and others to be amenable to carbon gains, although this is highly dependent on fire behavior and modeling uncertainties.

References

Aber, J., R. P. Neilson, S. McNulty, J. M. Lenihan, D. Bachelet, and R. J. Drapek. 2001. Forest processes and global environmental change: Predicting the effects of individual and multiple stressors. *Bioscience* 51, no. 9: 735-751.

Agee, J. K. 1993. *Fire ecology of Pacific Northwest forests*. Island Press Washington, DC (USA).

Bachelet, D., R. P. Neilson, J. M. Lenihan, and R. J. Drapek. 2001. Climate change effects on vegetation distribution and carbon budget in the United States. *Ecosystems* 4, no. 3 (April 21): 164-185. doi:10.1007/s10021-001-0002-7.

---. 2004. Regional differences in the carbon source-sink potential of natural vegetation in the U.S.A. *Environmental Management* 33, no. 0 (July 1): S23-S43. doi:10.1007/s00267-003-9115-4.

Bailey, R. G. 1995. Description of the ecoregions of the United States. *Miscellaneous publication/United States Department of Agriculture, Forest Service (USA)*.

Belsky, A. J. 1996. Viewpoint: Western juniper expansion: Is it a threat to arid northwestern ecosystems? *Journal of Range Management*: 53-59.

Blackard, J. A., M. V. Finco, E. H. Helmer, G. R. Holden, M. L. Hoppus, D. M. Jacobs, A. J. Lister, G. G. Moisen, M. D. Nelson, and R. Riemann. 2008. Mapping US forest biomass using nationwide forest inventory data and moderate resolution information. *Remote Sensing of Environment* 112, no. 4: 1658-1677.

Blate, G. M., L. A. Joyce, J. S. Littell, S. G. McNulty, C. I. Millar, S. C. Moser, R. P. Neilson, K. O'Halloran, and D. L. Peterson. 2009. Adapting to climate change in United States national forests.

Bonan, G. B. 1997. Effects of land use on the climate of the United States. *Climatic Change* 37, no. 3 (November 1): 449-486. doi:10.1023/A:1005305708775.

Bowman, D. M. J. S., J. K. Balch, P. Artaxo, W. J. Bond, J. M. Carlson, M. A. Cochrane, C. M. D'Antonio, R. S. DeFries, J. C. Doyle, and S. P. Harrison. 2009. Fire in the Earth system. *Science* 324, no. 5926: 481.

Campbell, J., D. Donato, D. Azuma, and B. Law. 2007. Pyrogenic carbon emission from a large wildfire in Oregon, United States. *J. Geophys. Res* 112: G04014.

CCSP. 2007. The First State of the Carbon Cycle Report (SOCCR). The North American Carbon Budget and Implications for the Global Carbon Cycle. In *A Report by the U.S. Climate Change Science Program and the Subcommittee on Global Change Research*, ed. A. W. King, L. Dilling, G. P. Zimmerman, D. M. Fairman, R. A. Houghton, G. Marland, A. Z. Rose, and Wilbanks, 242. Asheville, NC, USA: National Oceanic and Atmospheric Administratin, National Climatic Data Center.

Climate Impacts Group. 2004. *Overview of Climate Change Impacts in the U.S. Pacific Northwest*. Seattle, WA: University of Washington, July 29.

Climate Leadership Initiative, Institute for a Sustainable Environment. 2008. Preparing

the Pacific Northwest for Climate Change: A Framework for Integrative Preparation Planning for Natural, Human, Built and Economic Systems. University of Oregon.

Dale, V. H., L. A. Joyce, S. McNulty, R. P. Neilson, M. P. Ayres, M. D. Flannigan, P. J. Hanson, et al. 2001. Climate change and forest disturbances. (Cover story). *Bioscience* 51, no. 9: 723. doi:Article.

Daly, C., M. Halbleib, J. I. Smith, W. P. Gibson, M. K. Doggett, G. H. Taylor, J. Curtis, P. P. Pasteris, and N. USDA. 2008. Physiographically sensitive mapping of climatological temperature and precipitation across the conterminous United States.

Diaz-Nieto, J., and R. L. Wilby. 2005. A comparison of statistical downscaling and climate change factor methods: impacts on low flows in the River Thames, United Kingdom. *Climatic Change* 69, no. 2: 245-268.

Diffenbaugh, N. S., L. C. Sloan, M. A. Snyder, J. L. Bell, J. Kaplan, S. L. Shafer, and P. J. Bartlein. 2003. Vegetation sensitivity to global anthropogenic carbon dioxide emissions in a topographically complex region. *Global Biogeochemical Cycles* 17, no. 2: 1067.

Elsner, M. M. 2009. WashingtonState Climate Change Impacts Assessment: HB 1303 Key Findings presented at the The Washington Climate Change Impacts Assessment Conference, February 12, Washington State Convention Center, Seattle, Washington, U.S.A. http://cses.washington.edu/cig/outreach/waccia/index.html#Home.

Fowler, H. J., S. Blenkinsop, and C. Tebaldi. 2007. Linking climate change modelling to impacts studies: recent advances in downscaling techniques for hydrological modelling. *International Journal of Climatology* 27, no. 12: 1547-1578.

Galik, C. S., and R. B. Jackson. 2009. Risks to forest carbon offset projects in a changing climate. *Forest Ecology and Management*.

Gavin, D. G., D. J. Hallett, F. S. Hu, K. P. Lertzman, S. J. Prichard, K. J. Brown, J. A. Lynch, P. Bartlein, and D. L. Peterson. 2007. Forest fire and climate change in western North America: insights from sediment charcoal records. *Frontiers in Ecology and the Environment* 5, no. 9: 499-506.

Gordon, H. B. 2002. *The CSIRO Mk3 Climate System Model*. CSIRO Atmospheric Research Technical Paper No. 60. CSIRO Atmospheric Research.

Graham, R.T., A.E. Harvey, T.B. Jain, and J.R. Tonn. 1999. The effects of thinning and similar stand treatements on fire behavior in Western forests. In *Gen. Tech. Rep. PNW-GTR-463.*, 27. Portland, Oregon, USA: U.S. Department of Agriculture, Forest Service, Pacific Northwest Reserach Station.

von Hagen, B. 2009. Unexplored potentials of Northwest forests. In *Old Growth in a New World*, ed. T. A. Spies and Sally L. Duncan, 286-299. Washington, DC: Island Press.

Harr, R. D. 1977. Water flux in soil and subsoil on a steep forested slope. *Journal of*

Hydrology 33, no. 1/2.

Hasumi, H., and S. Emori, eds. 2004. K-1 Coupled GCM (MIROC) description. K-1 Model Developers Tech. rep. 1, 34 pp.

Hessl, A. E., D. McKenzie, and R. Schellhaas. 2008. Drought and Pacific Decadal Oscillation linked to fire occurrence in the inland Pacific Northwest. Research-article. September 12. http://www.esajournals.org/doi/abs/10.1890/03-5019.

IPCC. 2000. *Special Report on Emission Scenarios*. Ed. N. Nakicenovic and R. Swart. Cambridge, England: Cambridge University Press.

---. 2007. Climate Change 2007: Impacts, Adaptation and Vulnerability. *Contribution of the Working Group II to the Fourth Assessment report of the Intergovernmental Panel on Climate Change*.

Jackson, S. T., and J. T. Overpeck. 2000. Responses of plant populations and communities to environmental changes of the late Quaternary. *Paleobiology* 26, no. sp4: 194-220.

Johns, T. C., J. M. Gregory, W. J. Ingram, C. E. Johnson, A. Jones, J. A. Lowe, J. F. B. Mitchell, D. L. Roberts, D. M. H. Sexton, and D. S. Stevenson. 2003. Anthropogenic climate change for 1860 to 2100 simulated with the HadCM3 model under updated emissions scenarios. *Climate Dynamics* 20, no. 6: 583-612.

Jones, J. A., and G. E. Grant. 1996. Peak flow responses to clear-cutting and roads in small and large basins, western Cascades, Oregon. *Water Resources Research* 32, no. 4: 959-974.

Keane, R. E. , J. K. Agee, P. Fulé, J. E. Keeley, C. Key, S. G. Kitchen, R. Miller, and L. A. Schulte. 2008. Ecological effects of large fires on US landscapes: benefit or catastrophe? *Int. J. Wildland Fire* 17, no. 6 (December 12): 696-712 .

Kern, J. S. 1995. Geographic patterns of soils water-holding capacity in the contiguous United States. *Soil Science Society of America* 59, no. 4: 1126-1133.

---. 2000. Geographic patterns of soil water-holding capacity in the contiguous United States. *Soil Science Society of America* 64, no. 1: 382-382.

Kittel, T. G. F., N. A. Rosenbloom, T. H. Painter, and D. S. Schimel. 1995. The VEMAP integrated database for modelling United States ecosystem/vegetation sensitivity to climate change. *Journal of Biogeography*: 857-862.

Koch, G. W., H. A. Mooney, J. S. Amthor, and G. W. Koch, eds. 1996. *Carbon dioxide and terrestrial ecosystems*. San Diego, CA: Academic Press.

Kuchler, A. 1975. Potential Natural Vegetation of the United States. 2nd edition. New York, NY: American Geographic Society.

Landsberg, J. J., and R. H. Waring. 1997. A generalised model of forest productivity using simplified concepts of radiation-use efficiency, carbon balance and partitioning. *Forest Ecology and Management* 95, no. 3: 209-228.

Law, B. E., O. J. Sun, J. Campbell, S. Van Tuyl, and P. E. Thornton. 2003. Changes in carbon storage and fluxes in a chronosequence of ponderosa pine. *Global Change*

Biology 9, no. 4: 510-524.

Lenihan, J. M., C. Daly, D. Bachelet, and R. P. Neilson. 1998. Simulating broad-scale fire severity in a dynamic global vegetation model. *Northwest Science* 72, no. 4: 91–101.

Linacre, E. T. 1977. A simple formula for estimating evaporation rates in various climates, using temperature data alone. *Agricultural Meteorology* 18: 409 - 424.

Littell, J. S., E. E. Oneil, D. Mckenzie, J. A. Hicke, J. A. Lutz, R. A. Norheim, and M. M. Elsner. 2009. Forest ecosystems, disturbance, and climatic change in Washington State, USA. In *Washington Climate Change Impacts Assessment: Evaluating Washington's Future in a Changing Climate*. Seattle, WA: The Climate Impacts Group, University of Washington.

Maurer, E. P., and H. G. Hidalgo. 2008. Utility of daily vs. monthly large-scale climate data: an intercomparison of two statistical downscaling methods. *Hydrology and Earth System Sciences* 12, no. 2: 551-563.

McKenzie, D., Z. E. Gedalof, D. L. Peterson, and P. Mote. 2004. Climatic change, wildfire, and conservation. *Conservation Biology* 18, no. 4: 890-902.

McKenzie, D., D. L. Peterson, and J. S. Littell. 2009. Global warming and stress complexes in forests of western North America. In *Developments in Environmental Science: Wild Land Fires and Air Pollution*, 8:319-337. Amsterdam, The Netherlands: Elsevier Science, Ltd.

Meehl, G. A., C. Covey, T. Delworth, M. Latif, B. McAvaney, J. F. B. Mitchell, R. J. Stouffer, and K. E. Taylor. 2007. The WCRP CMIP3 multimodel dataset. *Bull. Am. Meteorol. Soc* 88: 1383–1394.

Miles, E. L., D. P. Lettenmaier, and et al. 2007. HB 1303 Interim Report: A Comprehensive Assessment of the Impacts of Climate Change on the State of Washington. University of Washington JISAO CSES Climate Impacts Group.

Millar, C. I., R. Neilson, D. Batchelet, R. Drapek, and J. Lenihan. 2006. Climate change at multiple scales. *Forests, carbon, and climate change: a synthesis of science findings. Oregon Forest Resources Institute, Portland, Oregon, USA*: 31–62.

Monteith, J. L. 1995. Accommodation between transpiring vegetation and the convective boundary layer. *Journal of Hydrology* 166, no. 3-4: 251-263.

Mote, P., E. Salathe, V. Duliere, and E. Jump. 2008. *Scenarios of Future Climate for the Pacific Northwest*. Seattle, WA: Climate Impacts Group, University of Washington.

Mote, Philip W., Edward A. Parson, Alan F. Hamlet, William S. Keeton, Dennis Lettenmaier, Nathan Mantua, Edward L. Miles, et al. 2003. Preparing for Climatic Change: The Water, Salmon, and Forests of the Pacific Northwest. *Climatic Change* 61, no. 1 (November 1): 45-88. doi:10.1023/A:1026302914358.

Nakicenovic, N., J. Alcamo, G. Davis, B. de Vries, J. Fenhann, S. Gaffin, K. Gregory, A. Grubler, T. Y. Jung, and T. Kram. 2000. *Special report on emissions scenarios: a special report of Working Group III of the Intergovernmental Panel on Climate*

Change. PNNL-SA-39650, Cambridge University Press, New York, NY (US).

Neilson, R. P. 1993. Transient ecotone response to climatic change: some conceptual and modelling approaches. *Ecological Applications*: 385-395.

Neilson, R.P. 2004. Impacts of climate change on Pacific Northwest terrestrial ecosystems. Oral Presentation presented at the Impacts of Climate Change on the Pacific Northwest Meeting, June 14, Corvallis, OR. http://inr.oregonstate.edu/presentations.html.

Neilson, Ronald P. 1995. A model for predicting continental-scale vegetation distribution and water balance. *Ecological Applications* 5, no. 2 (May): 362-385. doi:10.2307/1942028.

Norby, R. J., E. H. DeLucia, B. Gielen, C. Calfapietra, C. P. Giardina, J. S. King, J. Ledford, H. R. McCarthy, D. J. P. Moore, and R. Ceulemans. 2005. Forest response to elevated CO2 is conserved across a broad range of productivity. *Proceedings of the National Academy of Sciences* 102, no. 50: 18052-18056.

Norby, R. J., J. M. Warren, C. M. Iversen, B. E. Medlyn, R. E. McMurtrie, and F. M. Hoffman. 2008. Nitrogen limitation is reducing the enhancement of NPP by elevated CO2 in a deciduous forest. *EOS Trans. AGU* 89, no. 53. Fall Meet. Suppl., Abstract B32B-05.

NRCS (Natural Resources Conservation Service). 1994. State Soil Geographic (STATSGO) Data Base: data use information. In *Misc. Pub. Number 1492*. Lincoln, NE: USDA NRCS National Soil Survey Center.

Oregon Department of Forestry. Oregon.gov Home Page. http://www.oregon.gov/ODF/STATE_FORESTS/FRP/.

Overpeck, J., D. Rind, and R. Goldberg. 1990. Climate-induced changes in forest disturbance and vegetation. *Nature* 343: 51-53.

Parton, W., D. Schimel, D. Ojima, and C. Cole. 1994. A general study model for soil organic model dynamics, sensitivity to litter chemistry, texture, and management. *Soil Science Society of America* SSSA Special Publication 39: 147-167.

Pierce, D. W., T. P. Barnett, H. G. Hidalgo, T. Das, C. Bonfils, B. D. Santer, G. Bala, M. D. Dettinger, D. R. Cayan, and A. Mirin. 2008. Attribution of declining western US snowpack to human effects. *Journal of Climate* 21, no. 23: 6425-6444.

Raupach, Michael R., Gregg Marland, Philippe Ciais, Corinne Le Quéré, Josep G. Canadell, Gernot Klepper, and Christopher B. Field. 2007. Global and regional drivers of accelerating CO2 emissions. *Proceedings of the National Academy of Sciences* 104, no. 24 (June 12): 10288-10293. doi:10.1073/pnas.0700609104.

Root, T. L., J. T. Price, K. R. Hall, S. H. Schneider, C. Rosenzweig, and J. A. Pounds. 2003. Fingerprints of global warming on wild animals and plants. *Nature* 421, no. 6918: 57-60.

Running, S. W., R. R. Nemani, F. A. Heinsch, M. Zhao, M. Reeves, and H. Hashimoto. 2004. A continuous satellite-derived measure of global terrestrial primary production. *BioScience* 54, no. 6: 547-560.

Salathe Jr, E. P., P. W. Mote, and M. W. Wiley. 2007. Review of scenario selection and downscaling methods for the assessment of climate change impacts on hydrology in the United States pacific northwest. *International Journal of Climatology* 27, no. 12.

Scheller, R. M., and D. J. Mladenoff. 2007. An ecological classification of forest landscape simulation models: tools and strategies for understanding broad-scale forested ecosystems. *Landscape Ecology* 22, no. 4: 491-505.

Shafer, S. L., P. J. Bartlein, and R. S. Thompson. 2001. Potential changes in the distributions of western North America tree and shrub taxa under future climate scenarios. *Ecosystems* 4, no. 3 (April 21): 200-215. doi:10.1007/s10021-001-0004-5.

Smithwick, E. A. H., M. E. Harmon, S. M. Remillard, S. A. Acker, and J. F. Franklin. 2002. Potential upper bounds of carbon stores in forests of the Pacific Northwest. *Ecological applications* 12, no. 5: 1303-1317.

Spies, T. A., and J. F. Franklin. 1991. The structure of natural young, mature, and old-growth Douglas-fir forests in Oregon and Washington. In *Wildlife and vegetation of unmanaged Douglas-fir forests*, ed. L. F. Ruggiero, K. B. Aubry, A. B. Carey, and M. H. Huff, 91-111. 285th ed. Portland, Oregon, USA: USDA Forest Service Pacific Northwest Research Station.

Stephens, S. L., J. J. Moghaddas, C. Edminster, C. E. Fiedler, S. Haase, M. Harrington, J. E. Keeley, E. E. Knapp, J. D. McIver, and K. Metlen. 2009. Fire treatment effects on vegetation structure, fuels, and potential fire severity in western US forests. *Ecological Applications* 19, no. 2: 305-320.

Thompson, R. S., S. W. Hostetler, P. J. Bartlein, and K. H. Anderson. 1998. A strategy for assessing potential future changes in climate, hydrology, and vegetation in the western United States. *U. S. Geological Survey circular*, no. 1153: 1-20.

Thornton, P. E., S. C. Doney, K. Lindsay, J. K. Moore, N. Mahowald, J. T. Randerson, I. Fung, J. F. Lamarque, J. J. Feddema, and Y. H. Lee. 2009. Carbon-nitrogen interactions regulate climate-carbon cycle feedbacks: results from an atmosphere-ocean general circulation model. *Carbon* 6: 3303-3354.

Tuttle, A., and K. Andrasko. 2005. Registries and research: climate change mitigation and forestry in the United States. *UNASYLVA-FAO*- 56, no. 3: 42.

Van Mantgem, P. J., N. L. Stephenson, J. C. Byrne, L. D. Daniels, J. F. Franklin, P. Z. Fule, M. E. Harmon, A. J. Larson, J. M. Smith, and A. H. Taylor. 2009. Widespread increase of tree mortality rates in the western United States. *Science* 323, no. 5913: 521.

Van Tuyl, S., B. E. Law, D. P. Turner, and A. I. Gitelman. 2005. Variability in net primary production and carbon storage in biomass across Oregon forests—an assessment integrating data from forest inventories, intensive sites, and remote sensing. *Forest Ecology and Management* 209, no. 3: 273-291.

Walther, G. R., E. Post, P. Convey, A. Menzel, C. Parmesan, T. J. C. Beebee, J. M. Fromentin, O. Hoegh-Guldberg, and F. Bairlein. 2002. Ecological responses to

recent climate change. *Nature* 416, no. 6879: 389-395.

Washington State Department of Natural Resources. Washington State Timber Harvest. http://dnr.wa.gov/BusinessPermits/Topics/Budget/Pages/washington_state_timber_harvest.aspx.

Washington, W. M., and C. L. Parkinson. 2005. *An introduction to three-dimensional climate modeling*. University Science Books, February.

Westerling, A. L., T. J. Gershunov, T. J. Brown, D. R. Cayan, and M. D. Dettinger. 2003. Climate and wildfire in the western United States. *American Meteorological Society*: 595-603.

Whitely Binder, L. C. 2009. Preparing for climate change in the U.S. Pacific Northwest. *West-Northwest Journal of Environmental Law and Policy* 15, no. 1: 183-196.

Whitlock, C. 1992. Vegetational and climatic history of the Pacific Northwest during the last 20,000 years: implications for understanding present-day biodiversity. *Northwest Environmental Journal* 8: 5-5.

Whitlock, C., and M. A. Knox. 2002. Prehistoric burning in the Pacific Northwest: human versus climatic influences. *Fire, Native Peoples, and the Natural Landscape*: 195-231.

Whitlock, C., S. L. Shafer, and J. Marlon. 2003. The role of climate and vegetation change in shaping past and future fire regimes in the northwestern US and the implications for ecosystem management. *Forest Ecology and Management* 178, no. 1-2: 5-21.

Wullschleger, S. D., W. M. Post, and A. W. King. 1995. *Biotic feedbacks in the global climatic system*. Ed. G. M. Woodwell and F, T. Mackenzie. New York, NY: Oxford University Press US.

Appendices

Appendix A. Changes to parameters and MC1 source code.

File, Function, Line	Change	Effect
eachyr.F, eachyr, 99	wdfxa = epnfa(INTCPT) + epnfa(SLOPE) * MIN(prcann, 80.0)	limits abiotic fixation of nitrogen in wet areas
grem.F, grem, 52	flfrem = mf_flfrem fdfrem(1) = mf_fdfrem(1) fdfrem(2) = mf_fdfrem(2)	uses exact fire-induced grass carbon removal values passed from mapss instead of parameterizing
killrt.F, killrt, 44	fd(1) = mf_fd(1) fd(2) = mf_fd(2)	uses exact fire-induced root carbon removal values passed from mapss instead of parameterizing

wdeath.F, wdeath, 68	lfdr = mf_dr(1) + leafdr(month)
	wddrfb = mf_dr(2) + wooddr(FBRCH)
	wddrcw = mf_dr(3) + wooddr(LWOOD)
	if (lfdr .ge. 1.0) lfdr = 0.99
	if (wddrfb .ge. 1.0) wddrfb = 0.99
	if (wddrcw .ge. 1.0) wddrcw = 0.99
		Adds mortality from fire to background rates, and checks to see it is not greater than 1.0

lifeform_rules.c, MixIndex, 1115-1145	float sum;
	float ppt_avg;
	for (mo=JAN; mo<=DEC; mo++) sum += data_point->ppt[mo];
	ppt_avg = sum/12.;
	p_hi = MAX(90,, ppt_avg);
		Modulates index that determines deciduous component by rest of growing season precipitation. Results in mostly evergreen needle-leave forests in Olympics and North Cascades regions.

mapss_1t.c, mapss_1t, 412	data_point->vemap2_mo.nb_vtype = 0;	initializes veg type at year 0
mapss_1t.c, mapss_1d, 749	data_point->fuel_data.clai[mo] = lai[mo][WOODY]	properly passes information on LAI values
newbiogeog.c, NewBiogeogLynx	*(contact author)*	restructured biogeography, changed thresholds

fuel_load.c, tree_dim, 153, 184, 197, 212	data_point->fuel_data.clai[mo] = tree_lai;
	tree_lai = data_point->fuel_data.clai[mo];
	(deleted) tree_lai = 5.5;
	(deleted) tree_lai = 5.5
		uses model-calculated LAI values for fuel load calculations

fire_eff.c, mortality, 248	if (prob_mort <= mort_thres) mort = FALSE;	resets variable 'mort' if fire intensity is low enough
fire_eff.c, consump, 339	for (i = 0; i < 4; i++) { if (killed[i] < 33) killed[i] = 33; }	makes lower limit for low intensity fires 33% of vegetation consumed within burn area
fire_occur.c, , vveg_thresLynx, 142	ffmc = 1.008*(*previous value*) (*repeats for all tree types*)	results in less frequent fires, especially for dry areas

fire_sched.c, FireSched, 121	cen_state[0] = data_point-fire_eff.consume[burn_day][1] * part;
	cen_state[1] = data_point-fire_eff.consume[burn_day][2] * part;
	cen_state[2] = data_point-fire_eff.consume[burn_day][2] * part;
	cen_state[3] = data_point-fire_eff.consume[burn_day][3] * part;
		passes dynamic calculation of vegetation consumed within burn area to century side. Uses root death rates from fire_eff.c

	cen_state[4] = data_point-
	fire_eff.consume[burn_day][5] * part;
	cen_state[5] = data_point-
	fire_eff.consume[burn_day][0] * part;
	cen_state[6] = data_point-
	fire_eff.consume[burn_day][3] * part;
	cen_state[7] = data_point-
	fire_eff.consume[burn_day][3] * part;
	cen_state[8] = data_point-
	fire_eff.turnover[burn_day][0] * part;
	cen_state[9] = data_point-
	fire_eff.turnover[burn_day][1] * part;
	cen_state[10] = data_point-
	fire_eff.turnover[burn_day][2] * part;
	cen_state[11] = data_point-
	fire_eff.turnover[burn_day][3] * part;
	cen_state[12] = data_point-
	fire_eff.turnover[burn_day][3] * part;
	for (I = 0; I < 13; i++) {
	if (cen_state[i] == 1.0)
	cen_state[i] = 0.999; }	

tree.100	*(contact author)*	reset many parameters to original values from century. Altered allocation and death parameters.

Appendix B. Climatic variables by region and scenario. Historical variables are annual means from 1971-2000, and future variables are annual means from 2070-2099.

Region	Scenario	Precipitation (mm H2O month^{-1})	Mean Temperature (°C)	Daily Minimum Temperature (°C)	Daily Maximum Temperature (°C)	Vapor Pressure Deficit (Pa)
Whole Domain	Historical	98.46	8.36	2.32	14.40	453.36
	CSIRO B1	101.97	9.78	3.80	15.90	523.92
	CSIRO A1B	108.23	10.11	4.30	16.04	520.44
	CSIRO A2	113.13	10.97	5.09	16.93	548.47
	MIROC B1	105.07	11.60	5.43	17.85	564.62
	MIROC A1B	105.21	12.26	6.08	18.55	577.62
	MIROC A2	105.32	12.57	6.32	18.93	595.29
	Hadley B1	94.48	11.24	4.68	17.24	644.77
	Hadley A1B	89.17	12.49	5.65	18.66	747.12
	Hadley A2	91.97	12.58	6.28	19.17	736.62
Western Forests	Historical	166.89	9.20	3.94	14.46	365.55
	CSIRO B1	171.69	10.55	5.30	15.84	425.30
	CSIRO A1B	182.75	10.86	5.78	15.96	417.98
	CSIRO A2	190.57	11.68	6.53	16.81	433.36
	MIROC B1	177.96	12.21	6.85	17.63	449.81
	MIROC A1B	178.34	12.79	7.43	18.23	451.36
	MIROC A2	178.68	13.03	7.62	18.53	461.23
	Hadley B1	158.04	11.88	6.11	17.10	528.97
	Hadley A1B	148.87	13.05	7.04	18.52	618.12
	Hadley A2	154.06	13.11	7.66	18.90	607.04
Eastern Forests	Historical	59.76	6.14	-0.26	12.53	447.26
	CSIRO B1	62.73	7.65	1.35	14.12	518.09
	CSIRO A1B	65.99	7.98	1.86	14.26	516.72
	CSIRO A2	69.51	8.88	2.69	15.19	552.79
	MIROC B1	63.94	9.53	3.01	16.18	565.46
	MIROC A1B	64.14	10.25	3.70	16.93	583.90
	MIROC A2	64.25	10.58	3.96	17.34	602.96
	Hadley B1	59.35	9.17	2.33	15.50	635.98
	Hadley A1B	56.41	10.47	3.32	16.96	735.23
	Hadley A2	57.92	10.56	3.95	17.52	726.04
Blue Mountains	Historical	39.82	6.37	-0.41	13.15	486.23
	CSIRO B1	42.08	7.89	1.21	14.85	556.53
	CSIRO A1B	43.55	8.21	1.69	15.02	557.18
	CSIRO A2	46.80	9.11	2.52	15.92	592.99
	MIROC B1	41.64	9.99	3.08	17.02	615.28
	MIROC A1B	41.10	10.79	3.85	17.89	640.47
	MIROC A2	40.82	11.23	4.19	18.42	668.47
	Hadley B1	40.36	9.59	2.19	16.24	686.23
	Hadley A1B	38.38	10.94	3.23	17.56	796.31

	Hadley A2	38.54	11.05	3.91	18.31	787.70
Coast Range	Historical	209.61	9.91	4.96	14.86	296.14
	CSIRO B1	213.39	11.14	6.20	16.11	348.40
	CSIRO A1B	228.91	11.45	6.67	16.24	339.09
	CSIRO A2	236.60	12.22	7.38	17.05	335.83
	MIROC B1	224.08	12.76	7.75	17.80	359.24
	MIROC A1B	224.21	13.29	8.28	18.35	353.59
	MIROC A2	224.96	13.50	8.45	18.61	359.34
	Hadley B1	195.02	12.35	6.93	17.23	432.02
	Hadley A1B	183.06	13.43	7.83	18.54	505.10
	Hadley A2	190.80	13.50	8.44	18.90	494.35
Columbia Plateau	Historical	24.58	8.84	1.88	15.80	592.57
	CSIRO B1	26.55	10.32	3.45	17.41	679.47
	CSIRO A1B	27.85	10.65	3.96	17.57	680.17
	CSIRO A2	29.35	11.56	4.79	18.50	721.15
	MIROC B1	26.28	12.30	5.19	19.52	739.61
	MIROC A1B	26.00	13.06	5.92	20.32	765.80
	MIROC A2	25.78	13.44	6.22	20.80	794.31
	Hadley B1	25.18	11.93	4.37	18.82	828.95
	Hadley A1B	23.89	13.26	5.37	20.24	953.98
	Hadley A2	24.07	13.36	6.02	20.88	943.31
East Cascades	Historical	69.37	6.28	-0.18	12.74	433.32
	CSIRO B1	73.06	7.76	1.34	14.31	505.50
	CSIRO A1B	76.70	8.09	1.84	14.46	505.77
	CSIRO A2	81.39	8.96	2.65	15.34	543.20
	MIROC B1	74.69	9.53	2.89	16.27	544.86
	MIROC A1B	74.76	10.22	3.55	17.00	562.20
	MIROC A2	75.19	10.55	3.81	17.41	579.92
	Hadley B1	69.01	9.31	2.33	15.70	615.14
	Hadley A1B	65.77	10.61	3.35	17.16	710.26
	Hadley A2	67.79	10.68	3.94	17.67	700.51
Klamath Mountains	Historical	122.82	10.95	4.63	17.26	559.97
	CSIRO B1	124.24	12.29	5.99	18.67	634.35
	CSIRO A1B	130.69	12.60	6.42	18.84	639.84
	CSIRO A2	143.87	13.37	7.18	19.58	691.80
	MIROC B1	124.74	13.76	7.36	20.18	676.18
	MIROC A1B	121.35	14.38	7.96	20.86	690.53
	MIROC A2	122.21	14.64	8.18	21.18	706.40
	Hadley B1	111.37	13.94	6.73	20.21	786.66
	Hadley A1B	104.62	15.26	7.81	21.87	925.30
	Hadley A2	106.94	15.28	8.27	22.08	910.04
North Cascades	Historical	237.93	5.87	1.33	10.40	321.57
	CSIRO B1	238.60	7.47	3.02	12.02	380.40
	CSIRO A1B	256.89	7.80	3.58	12.11	367.43
	CSIRO A2	259.58	8.73	4.38	13.12	393.17
	MIROC B1	252.39	9.42	4.78	14.21	421.10
	MIROC	259.74	10.01	5.39	14.77	423.08

	A1B					
	MIROC A2	260.09	10.23	5.55	15.04	430.81
	Hadley B1	228.76	8.60	3.95	13.40	479.28
	Hadley A1B	216.39	9.79	4.77	14.98	557.35
	Hadley A2	225.07	9.86	5.45	15.32	547.18
Okanagan	Historical	48.87	5.39	-0.37	11.15	452.12
	CSIRO B1	50.18	7.01	1.51	12.67	518.97
	CSIRO A1B	54.09	7.35	2.10	12.78	509.89
	CSIRO A2	53.95	8.36	3.01	13.85	541.65
	MIROC B1	51.75	9.07	3.33	14.97	581.10
	MIROC A1B	53.18	9.75	4.03	15.63	595.95
	MIROC A2	52.64	9.98	4.20	15.93	609.81
	Hadley B1	47.26	8.24	2.50	14.04	651.94
	Hadley A1B	44.28	9.53	3.31	15.65	753.44
	Hadley A2	45.54	9.64	4.03	16.17	745.54
West Cascades	Historical	163.92	7.75	2.32	13.17	369.45
	CSIRO B1	171.24	9.16	3.72	14.64	430.05
	CSIRO A1B	179.83	9.47	4.21	14.75	425.05
	CSIRO A2	190.43	10.31	4.98	15.61	449.81
	MIROC B1	174.40	10.82	5.25	16.46	460.32
	MIROC A1B	173.97	11.44	5.85	17.10	466.77
	MIROC A2	174.03	11.72	6.08	17.46	479.85
	Hadley B1	157.47	10.62	4.62	16.01	540.06
	Hadley A1B	148.84	11.84	5.60	17.42	632.17
	Hadley A2	152.78	11.92	6.21	17.88	622.43
Willamette Valley	Historical	104.37	10.83	5.60	16.05	374.68
	CSIRO B1	110.60	12.12	6.90	17.38	436.39
	CSIRO A1B	118.22	12.44	7.40	17.48	424.47
	CSIRO A2	121.85	13.27	8.14	18.36	429.06
	MIROC B1	114.86	13.83	8.50	19.23	455.65
	MIROC A1B	115.57	14.40	9.06	19.80	453.45
	MIROC A2	115.50	14.63	9.25	20.09	462.35
	Hadley B1	101.49	13.36	7.69	18.48	535.86
	Hadley A1B	95.54	14.48	8.58	19.84	622.36
	Hadley A2	98.92	14.57	9.24	20.26	610.68

Appendix C. Model output variables by scenario and region. Historical variables are annual means from 1971-2000, and future variables are annual means from 2070-2099.

Ecoregion	Scenario	Live Grass Carbon (g C m^{-2})	Live Tree Carbon (kg C m^{-2})	Dead Carbon (kg C m^{-2})	Total Ecosystem Carbon (kg C m^{-2})	Biomass Consumed by Fire (g C m^{-2} y^{-1})
Whole Domain	Historical	31.40	13.61	14.08	27.71	16.54
	CSIRO B1	34.97	13.05	14.49	27.57	35.46
	CSIRO A1B	36.86	12.62	14.47	27.13	23.38
	CSIRO A2	39.04	12.90	14.51	27.45	31.53
	MIROC B1	33.08	14.00	14.09	28.13	15.63
	MIROC A1B	34.59	13.64	14.20	27.88	19.77
	MIROC A2	34.49	13.42	14.37	27.83	25.20
	Hadley B1	32.25	9.46	14.96	24.45	54.04
	Hadley A1B	32.70	8.06	15.06	23.15	61.36
	Hadley A2	32.54	8.26	15.21	23.50	62.42
Western Forests	Historical	1.94	25.39	20.73	46.12	6.57
	CSIRO B1	2.21	24.08	21.46	45.53	39.89
	CSIRO A1B	2.27	23.05	21.37	44.42	16.90
	CSIRO A2	3.69	23.55	21.51	45.06	30.71
	MIROC B1	2.20	25.15	20.68	45.83	5.02
	MIROC A1B	2.51	24.68	20.85	45.53	7.77
	MIROC A2	2.57	24.47	21.06	45.53	14.67
	Hadley B1	2.41	17.03	22.53	39.56	83.01
	Hadley A1B	4.42	14.06	22.72	36.78	98.61
	Hadley A2	4.10	14.46	23.02	37.48	100.66
Eastern Forests	Historical	24.54	7.26	13.38	20.66	41.57
	CSIRO B1	23.26	7.20	13.65	20.87	54.41
	CSIRO A1B	24.67	7.32	13.72	21.06	46.42
	CSIRO A2	25.48	7.55	13.65	21.22	54.23
	MIROC B1	21.07	9.20	13.43	22.65	38.68
	MIROC A1B	22.95	8.64	13.58	22.25	49.34
	MIROC A2	23.11	8.12	13.83	21.97	59.54
	Hadley B1	22.49	5.75	13.58	19.35	52.24
	Hadley A1B	22.45	5.64	13.60	19.26	52.67
	Hadley A2	22.18	5.69	13.66	19.38	53.38
Blue Mountains	Historical	19.11	4.89	13.94	18.85	46.49
	CSIRO B1	19.39	5.80	14.21	20.03	46.51
	CSIRO A1B	20.82	5.97	14.33	20.32	45.44
	CSIRO A2	20.00	6.13	14.26	20.41	45.04
	MIROC B1	16.34	6.02	14.34	20.38	47.65
	MIROC A1B	17.56	5.74	14.37	20.12	49.17
	MIROC A2	16.34	5.70	14.47	20.19	46.68
	Hadley B1	20.99	5.10	14.08	19.20	45.00
	Hadley A1B	20.38	5.10	14.13	19.26	45.27
	Hadley A2	19.98	5.06	14.15	19.23	45.23

Coast Range	Historical	0.88	28.22	21.22	49.44	0.37
	CSIRO B1	0.73	27.23	21.68	48.90	7.14
	CSIRO A1B	0.83	26.90	21.63	48.53	3.63
	CSIRO A2	0.89	26.91	21.70	48.61	9.08
	MIROC B1	1.05	27.32	21.27	48.59	0.03
	MIROC A1B	1.06	26.96	21.38	48.34	0.01
	MIROC A2	1.03	26.93	21.48	48.41	0.12
	Hadley B1	0.76	23.04	22.60	45.64	48.57
	Hadley A1B	2.13	19.68	23.36	43.04	86.28
	Hadley A2	0.94	19.90	23.52	43.42	83.05
Columbia Plateau	Historical	80.45	0.89	4.64	5.61	11.88
	CSIRO B1	92.81	1.09	4.68	5.86	14.25
	CSIRO A1B	97.80	1.13	4.70	5.92	15.02
	CSIRO A2	102.07	1.11	4.68	5.89	14.99
	MIROC B1	88.37	1.05	4.71	5.85	13.53
	MIROC A1B	91.44	1.01	4.71	5.81	14.66
	MIROC A2	91.01	1.01	4.74	5.84	14.16
	Hadley B1	84.00	0.95	4.69	5.72	12.42
	Hadley A1B	82.43	0.91	4.69	5.69	12.13
	Hadley A2	82.73	0.90	4.69	5.67	12.10
East Cascades	Historical	25.37	7.76	13.61	21.39	46.02
	CSIRO B1	20.71	7.80	13.75	21.57	57.36
	CSIRO A1B	21.83	7.86	13.85	21.73	48.41
	CSIRO A2	23.14	8.04	13.75	21.81	56.69
	MIROC B1	18.84	10.42	13.49	23.92	36.94
	MIROC A1B	20.45	9.71	13.67	23.40	50.68
	MIROC A2	20.11	9.13	13.94	23.08	63.71
	Hadley B1	20.83	6.08	13.72	19.82	55.21
	Hadley A1B	20.45	6.01	13.72	19.75	55.49
	Hadley A2	20.16	6.06	13.82	19.90	56.39
Klamath Mountains	Historical	10.65	15.39	20.81	36.21	26.51
	CSIRO B1	12.26	14.30	21.21	35.53	39.65
	CSIRO A1B	12.97	14.19	21.38	35.58	43.92
	CSIRO A2	13.73	13.97	21.12	35.10	45.00
	MIROC B1	12.63	15.86	20.38	36.25	22.60
	MIROC A1B	13.20	15.18	20.53	35.72	27.42
	MIROC A2	12.96	14.93	20.85	35.80	37.21
	Hadley B1	11.81	10.54	21.34	31.90	74.97
	Hadley A1B	11.87	8.86	21.29	30.15	86.23
	Hadley A2	12.00	9.24	21.66	30.91	89.93
North Cascades	Historical	0.83	20.04	15.13	35.17	0.95
	CSIRO B1	2.82	17.28	16.25	33.53	70.61
	CSIRO A1B	1.56	16.11	15.80	31.91	14.98
	CSIRO A2	16.04	14.93	16.72	31.66	58.36
	MIROC B1	0.78	21.37	14.84	36.21	3.89
	MIROC A1B	3.17	21.07	14.96	36.03	9.14

	MIROC A2	4.38	20.60	15.14	35.75	26.38
	Hadley B1	5.31	10.40	16.72	27.13	101.28
	Hadley A1B	21.37	8.66	16.30	24.98	90.37
	Hadley A2	21.42	8.90	16.65	25.57	99.76
Okanagan	Historical	27.60	8.12	11.97	20.12	21.17
	CSIRO B1	36.11	6.68	12.72	19.43	52.99
	CSIRO A1B	38.46	6.94	12.65	19.62	40.75
	CSIRO A2	39.31	7.44	12.66	20.13	55.89
	MIROC B1	33.73	8.56	12.24	20.83	34.83
	MIROC A1B	37.29	8.19	12.43	20.66	44.99
	MIROC A2	40.58	7.36	12.76	20.15	59.38
	Hadley B1	29.71	5.31	12.56	17.90	50.03
	Hadley A1B	31.44	5.00	12.61	17.64	51.19
	Hadley A2	31.42	5.12	12.60	17.75	52.04
West Cascades	Historical	0.92	24.19	19.73	43.92	11.78
	CSIRO B1	0.66	23.05	20.52	43.57	49.48
	CSIRO A1B	0.78	21.39	20.57	41.96	29.66
	CSIRO A2	0.74	23.07	20.42	43.48	36.82
	MIROC B1	0.74	25.08	19.67	44.75	7.42
	MIROC A1B	0.76	24.47	19.92	44.39	13.32
	MIROC A2	0.73	24.12	20.15	44.27	27.48
	Hadley B1	0.82	13.17	21.91	35.08	98.32
	Hadley A1B	0.91	11.25	21.66	32.91	98.68
	Hadley A2	1.07	11.61	21.96	33.57	102.44
Willamette Valley	Historical	0.84	30.65	23.84	54.49	0.02
	CSIRO B1	0.98	29.16	24.85	54.01	57.87
	CSIRO A1B	1.15	27.66	24.53	52.20	4.29
	CSIRO A2	1.11	28.29	25.05	53.34	32.34
	MIROC B1	1.11	28.67	23.99	52.66	0.00
	MIROC A1B	1.20	28.29	24.14	52.42	0.00
	MIROC A2	1.15	28.16	24.44	52.60	0.08
	Hadley B1	0.82	20.40	26.43	46.83	104.75
	Hadley A1B	1.27	15.31	26.86	42.16	125.17
	Hadley A2	1.04	16.12	27.26	43.39	128.01

Appendix C (cont.)

Ecoregion	Scenario	Burn Area (% area burned per year)	Tree NPP (g C m^{-2} y^{-1})	Grass NPP (g C m^{-2} y^{-1})	Heterotrophic Respiration (g C m^{-2} yr^{-1})	Net Biome Production (g C m^{-2} y^{-1})
Whole Domain	Historical	2.20	400.56	18.97	404.30	-1.31
	CSIRO B1	3.81	420.27	20.23	431.06	-26.01
	CSIRO A1B	3.72	446.72	21.29	455.29	-10.66
	CSIRO A2	3.93	447.14	22.79	458.02	-19.61
	MIROC B1	3.02	438.74	20.00	444.31	-1.20
	MIROC A1B	3.32	437.17	20.84	447.00	-8.75
	MIROC A2	3.38	423.41	20.67	441.26	-22.38
	Hadley B1	3.46	379.72	19.75	409.16	-63.74
	Hadley A1B	3.54	373.82	20.02	410.18	-77.71
	Hadley A2	3.45	372.65	20.07	410.25	-79.95
Western Forests	Historical	0.23	664.89	1.03	656.55	2.80
	CSIRO B1	0.94	667.82	1.18	683.42	-54.31
	CSIRO A1B	0.46	709.12	1.19	720.98	-27.58
	CSIRO A2	0.76	702.69	1.92	723.63	-49.73
	MIROC B1	0.21	706.59	1.21	716.45	-13.67
	MIROC A1B	0.27	703.64	1.36	719.54	-22.30
	MIROC A2	0.43	681.78	1.41	710.46	-41.94
	Hadley B1	1.69	604.80	1.32	657.82	-134.71
	Hadley A1B	2.02	594.98	2.33	663.01	-164.31
	Hadley A2	2.02	590.61	2.16	662.69	-170.59
Eastern Forests	Historical	2.69	327.63	14.51	311.05	-10.47
	CSIRO B1	3.65	388.34	12.72	354.48	-7.83
	CSIRO A1B	3.41	413.53	13.45	376.11	4.46
	CSIRO A2	3.67	426.95	14.07	379.39	7.40
	MIROC B1	3.14	398.33	12.03	351.03	20.65
	MIROC A1B	3.54	398.64	13.05	354.50	7.86
	MIROC A2	3.69	383.69	13.11	349.01	-11.75
	Hadley B1	3.45	353.32	13.16	323.98	-9.74
	Hadley A1B	3.53	353.76	12.89	322.06	-8.08
	Hadley A2	3.49	357.38	12.89	323.13	-6.25
Blue	Historical	2.78	314.10	11.65	285.48	-6.23

Mountains						
	CSIRO B1	3.34	384.84	11.00	334.05	15.28
	CSIRO A1B	3.27	407.68	11.64	352.84	21.04
	CSIRO A2	3.25	426.72	11.55	361.05	32.18
	MIROC B1	3.15	382.49	9.80	328.08	16.55
	MIROC A1B	3.29	382.78	10.49	330.22	13.88
	MIROC A2	3.09	377.16	9.84	327.92	12.40
	Hadley B1	3.16	334.45	12.36	295.68	6.14
	Hadley A1B	3.19	335.57	11.94	296.60	5.64
	Hadley A2	3.11	337.98	11.82	294.94	9.63
Coast Range	Historical	0.01	740.60	0.32	734.82	5.73
	CSIRO B1	0.14	733.06	0.28	742.40	-16.20
	CSIRO A1B	0.07	775.68	0.31	784.89	-12.52
	CSIRO A2	0.18	772.45	0.34	786.37	-22.66
	MIROC B1	0.00	781.53	0.44	801.57	-19.64
	MIROC A1B	0.00	779.56	0.45	802.86	-22.86
	MIROC A2	0.00	761.82	0.44	794.60	-32.46
	Hadley B1	0.90	676.04	0.33	714.98	-87.18
	Hadley A1B	1.60	652.64	1.20	734.23	-166.67
	Hadley A2	1.52	649.23	0.45	726.93	-160.30
Columbia Plateau	Historical	4.68	59.78	49.16	97.39	-0.32
	CSIRO B1	8.22	72.81	54.46	111.14	1.87
	CSIRO A1B	8.86	78.06	57.36	117.46	2.94
	CSIRO A2	8.88	78.51	60.66	119.77	4.41
	MIROC B1	7.10	67.41	54.25	107.60	0.53
	MIROC A1B	7.70	66.43	56.00	109.00	-1.23
	MIROC A2	7.55	65.84	55.36	108.26	-1.22
	Hadley B1	6.04	60.70	52.25	101.06	-0.53
	Hadley A1B	5.75	56.39	51.75	98.22	-2.21
	Hadley A2	5.49	55.95	52.23	97.87	-1.79
East Cascades	Historical	2.81	340.75	14.30	327.22	-18.19
	CSIRO B1	3.47	406.04	11.21	369.28	-9.39
	CSIRO A1B	3.18	428.63	11.76	389.58	2.39
	CSIRO A2	3.49	443.79	12.62	393.02	6.71
	MIROC B1	2.81	421.77	10.61	368.95	26.50
	MIROC	3.31	419.33	11.53	371.19	8.99

	A1B					
	MIROC A2	3.57	403.34	11.33	365.13	-14.18
	Hadley B1	3.39	376.55	11.83	342.76	-9.59
	Hadley A1B	3.42	379.56	11.60	342.34	-6.66
	Hadley A2	3.39	382.37	11.63	343.66	-6.06
Klamath Mountains	Historical	1.33	573.86	6.35	556.27	-2.57
	CSIRO B1	1.64	597.31	7.15	587.10	-22.28
	CSIRO A1B	1.70	623.02	7.55	614.55	-27.91
	CSIRO A2	1.77	636.63	7.94	619.37	-19.79
	MIROC B1	1.28	607.81	7.51	601.30	-8.58
	MIROC A1B	1.37	603.04	7.77	605.76	-22.37
	MIROC A2	1.55	581.79	7.65	595.60	-43.36
	Hadley B1	2.42	561.92	6.98	567.66	-73.72
	Hadley A1B	2.71	529.32	7.14	548.09	-97.86
	Hadley A2	2.73	531.34	7.27	559.95	-111.28
North Cascades	Historical	0.03	489.58	0.34	490.23	-1.26
	CSIRO B1	1.75	482.70	1.44	525.68	-112.15
	CSIRO A1B	0.36	529.16	0.64	550.17	-35.35
	CSIRO A2	1.34	493.69	8.06	561.09	-117.70
	MIROC B1	0.11	572.41	0.39	553.07	15.84
	MIROC A1B	0.24	570.77	1.60	554.49	8.74
	MIROC A2	0.71	547.23	2.29	545.45	-22.30
	Hadley B1	2.37	470.37	2.79	511.58	-139.70
	Hadley A1B	2.53	478.43	9.91	501.52	-103.54
	Hadley A2	2.78	465.03	10.35	500.85	-125.23
Okanagan	Historical	2.18	297.97	18.32	284.10	11.02
	CSIRO B1	4.57	332.29	19.71	326.61	-27.61
	CSIRO A1B	4.31	368.83	21.14	355.76	-6.54
	CSIRO A2	4.70	370.25	21.73	353.18	-17.10
	MIROC B1	4.22	336.24	19.24	315.33	5.32
	MIROC A1B	4.60	345.88	20.99	324.40	-2.51
	MIROC A2	4.73	324.33	22.66	317.35	-29.74
	Hadley B1	3.96	295.22	18.50	291.15	-27.46
	Hadley A1B	4.29	286.25	18.29	281.08	-27.74
	Hadley A2	4.21	293.93	18.31	284.30	-24.10
West Cascades	Historical	0.29	601.01	0.44	591.48	-1.82

	CSIRO B1	1.13	608.30	0.31	621.90	-62.77
	CSIRO A1B	0.68	635.69	0.36	649.13	-42.75
	CSIRO A2	0.86	646.16	0.34	655.41	-45.74
	MIROC B1	0.19	656.89	0.36	651.29	-1.46
	MIROC A1B	0.33	649.70	0.37	650.92	-14.17
	MIROC A2	0.65	629.74	0.37	645.78	-43.14
	Hadley B1	1.98	538.63	0.41	598.39	-157.67
	Hadley A1B	2.04	559.32	0.47	608.95	-147.84
	Hadley A2	2.06	552.75	0.54	604.12	-153.27
Willamette Valley	Historical	0.00	773.45	0.41	764.07	9.76
	CSIRO B1	1.07	778.35	0.46	806.52	-85.58
	CSIRO A1B	0.08	842.93	0.54	862.60	-23.41
	CSIRO A2	0.62	811.04	0.53	857.06	-77.83
	MIROC B1	0.00	782.51	0.57	821.07	-37.99
	MIROC A1B	0.00	784.49	0.61	831.46	-46.35
	MIROC A2	0.00	754.80	0.59	816.30	-60.99
	Hadley B1	1.69	680.30	0.42	772.33	-196.36
	Hadley A1B	1.97	650.30	0.72	770.19	-244.34
	Hadley A2	1.95	648.37	0.56	779.59	-258.67

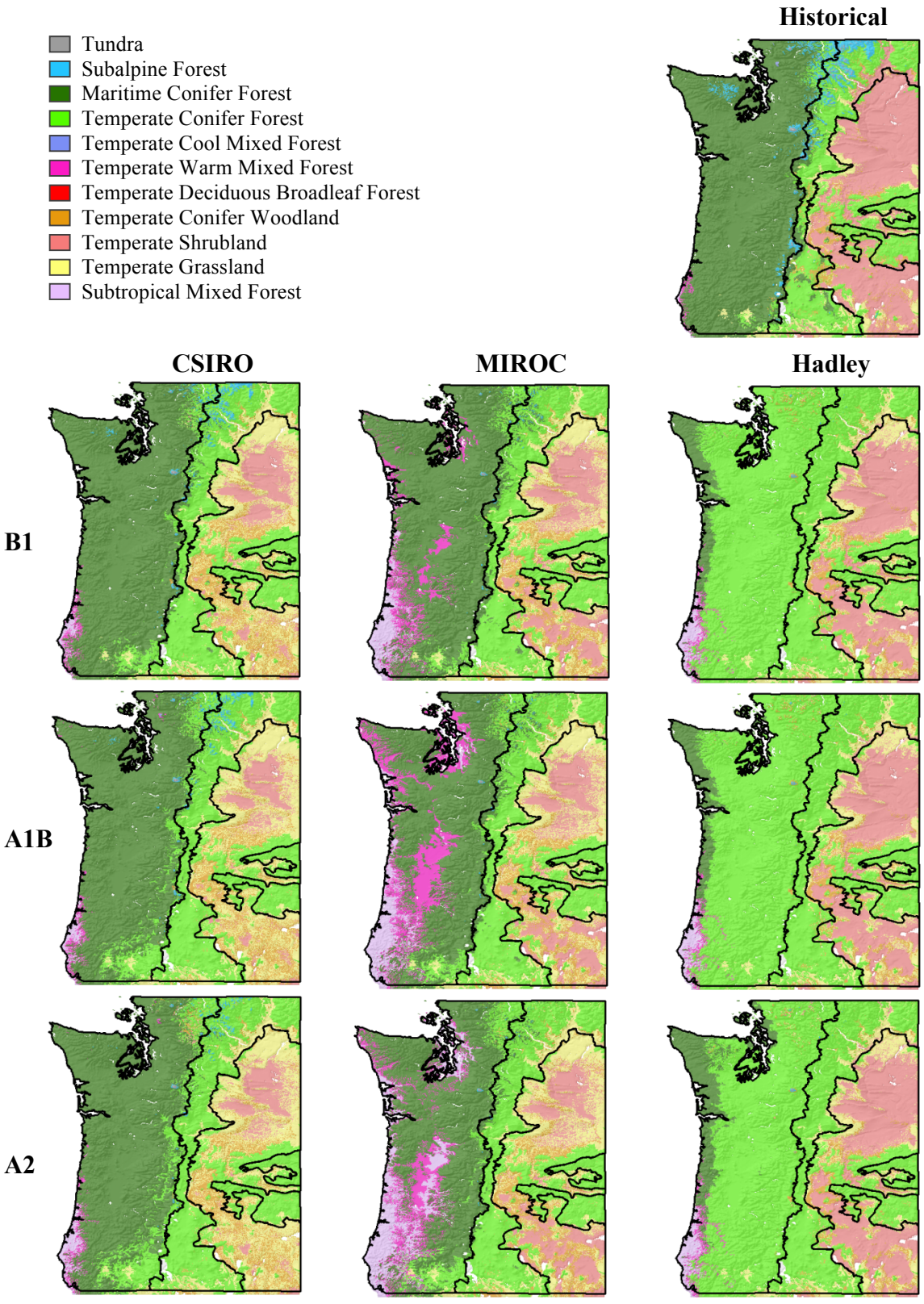

Appendix D. Mode vegetation types for historical (1971-2000) and future (2070 – 2099) MC1 simulations.

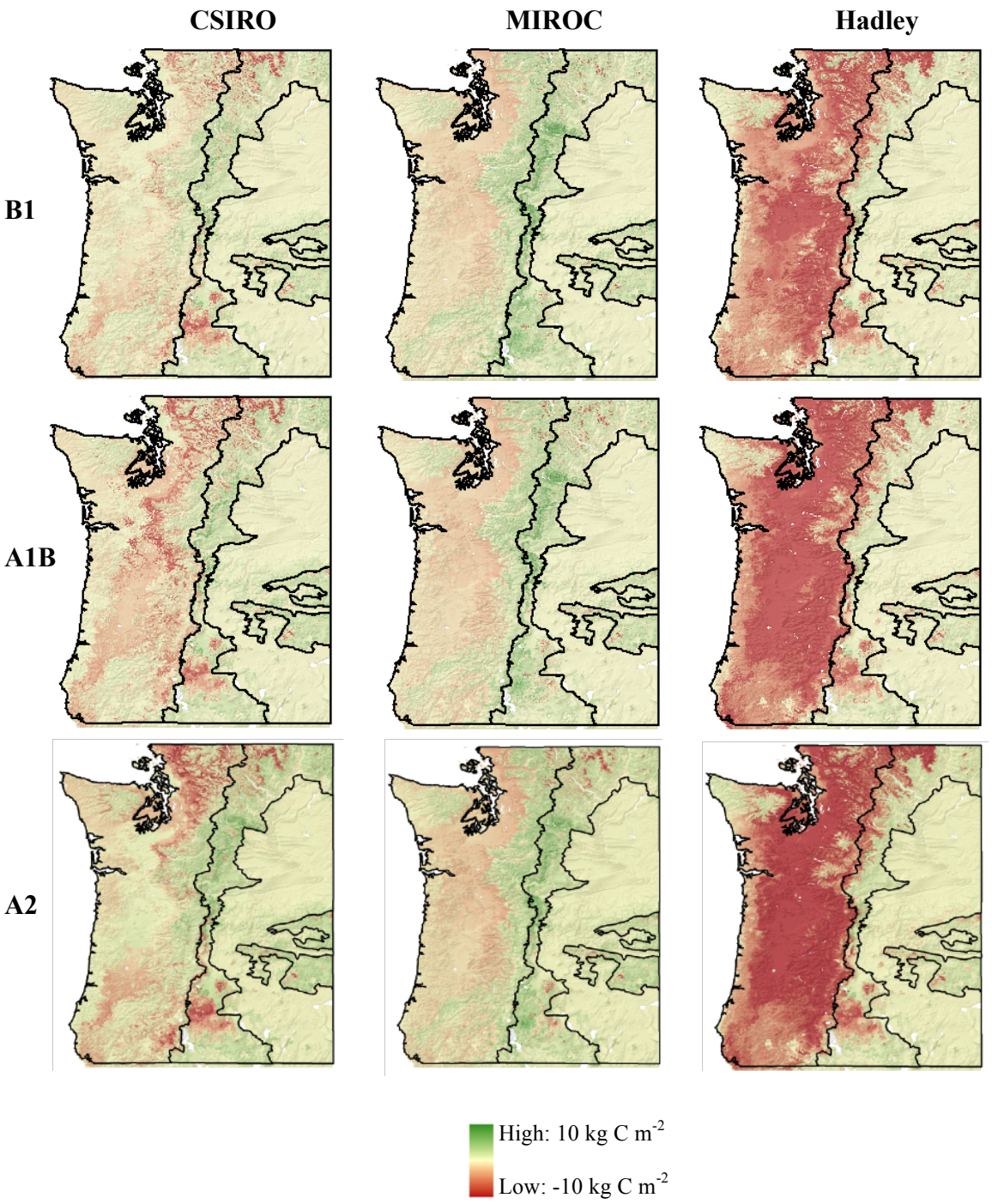

Appendix E. Mean changes in ecosystem carbon between historical (1971-2000) and future (2070 – 2099) MC1 simulations.

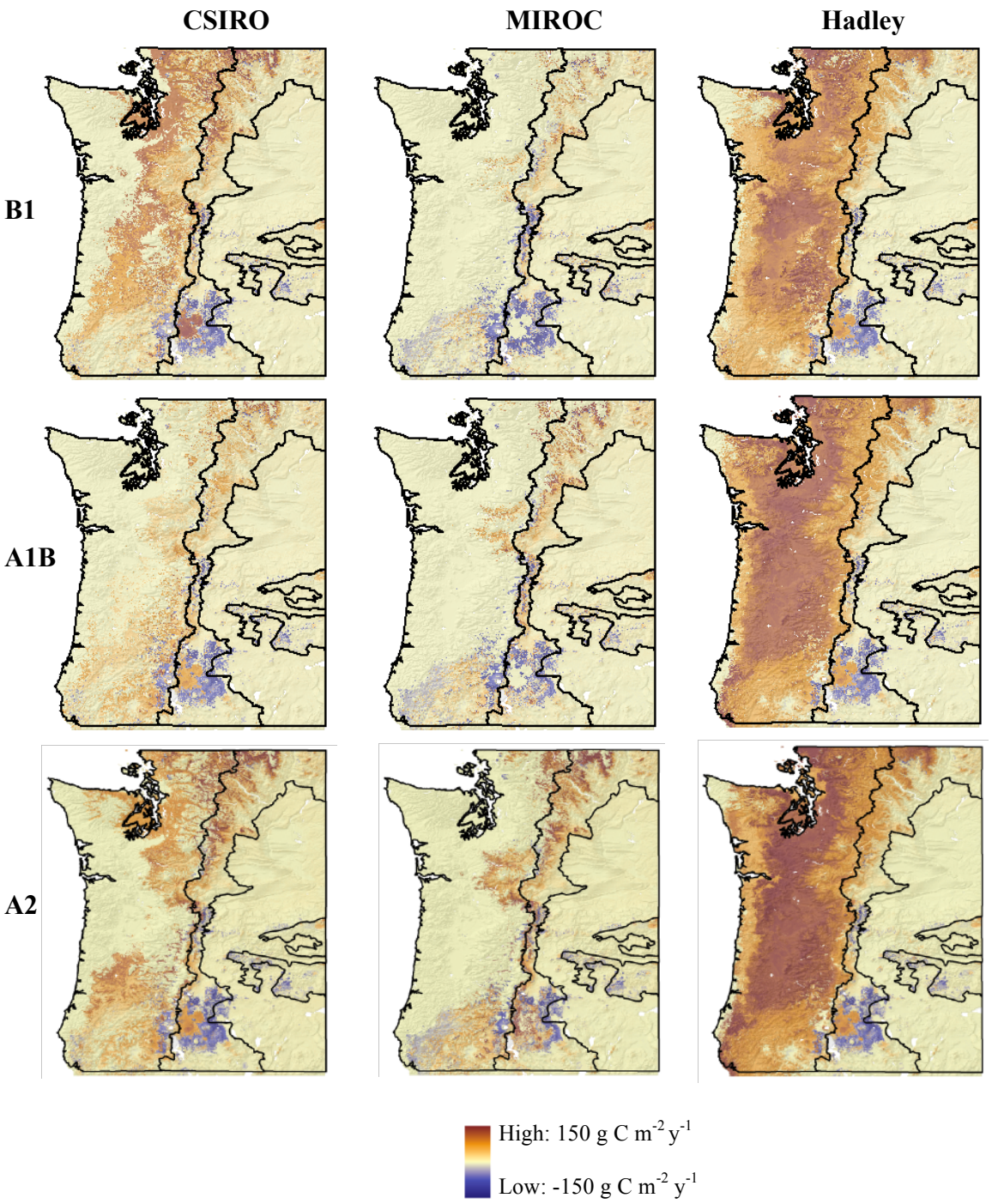

Appendix F. Mean changes in biomass consumed by fire between historical (1971-2000) and future (2070 – 2099) MC1 simulations.

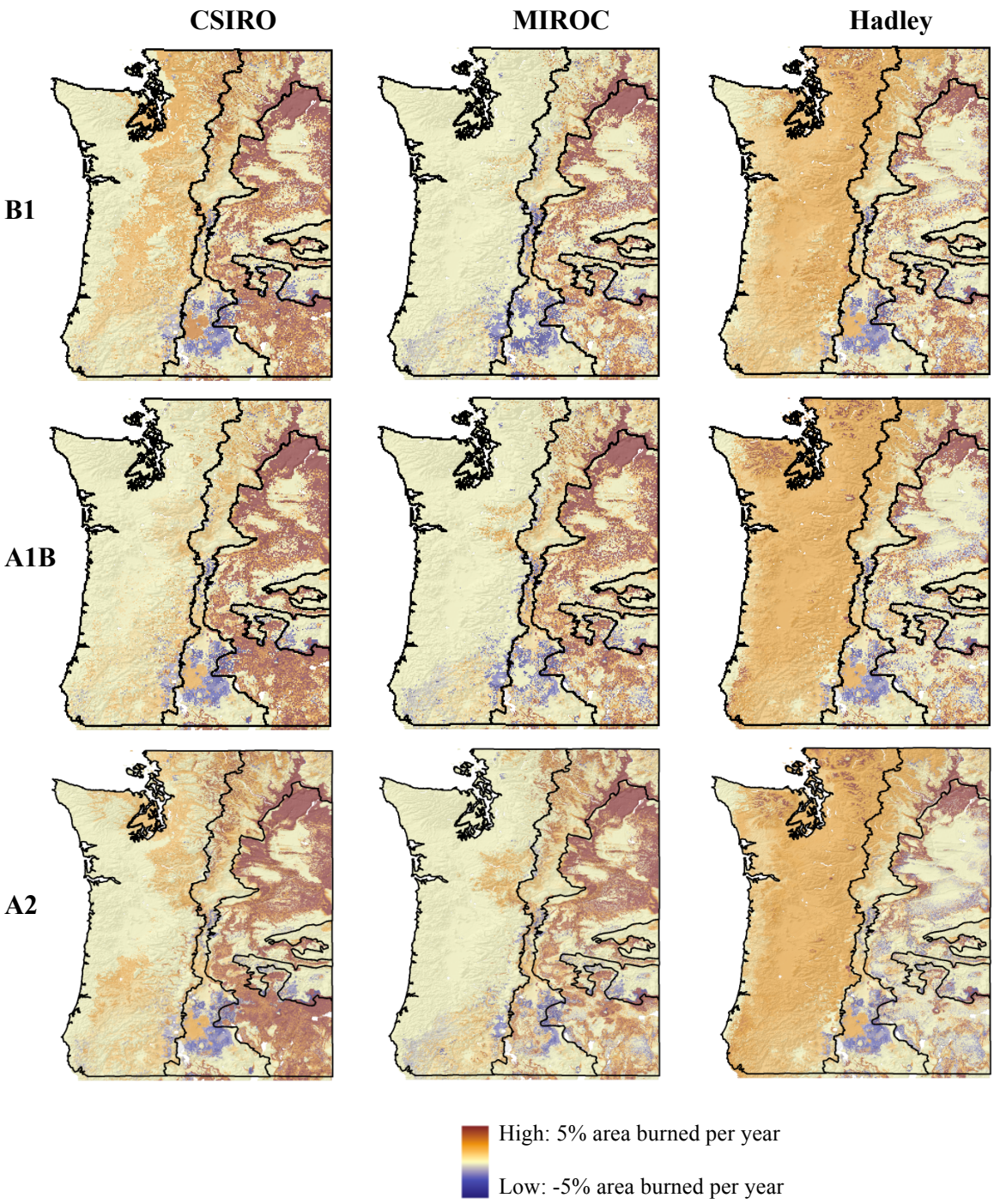

Appendix G. Mean changes in area burned between historical (1971-2000) and future (2070 – 2099) MC1 simulations.